STRUCTURAL ANALYSIS METHODS DEVELOPMENT FOR TURBINE HOT SECTION COMPONENTS

R. L. Thompson
National Aeronautics and Space Administration
Lewis Research Center
Cleveland, Ohio

ABSTRACT

This paper summarizes the structural analysis technologies and activities of the NASA Lewis Research Center's gas turbine engine Hot Section Technology (HOST) program. The technologies synergistically developed and validated include: time-varying thermal/mechanical load models; component-specific automated geometric modeling and solution strategy capabilities; advanced inelastic analysis methods; inelastic constitutive models; high-temperature experimental techniques and experiments; and nonlinear structural analysis codes. Features of the program that incorporate the new technologies and their application to hot section component analysis and design are described. Improved and, in some cases, first-time three-dimensional nonlinear structural analyses of hot section components of isotropic and anisotropic nickel-base superalloys are presented.

INTRODUCTION

Hot section components of aircraft gas turbine engines are subjected to severe thermal-structural loading conditions during the engine mission cycle. The most severe and damaging stresses and strains are those induced by the steep thermal gradients which occur during the startup and shutdown transients. The transient, as well as steady state, stresses and strains are difficult to predict, in part, because the temperature gradients and distributions are not well known or readily predictable and, in part, because the cyclic elastic-viscoplastic behavior of the materials at these extremes of temperature and strain are not well known or readily predictable.

A broad spectrum of structures related technology programs has been underway at the NASA Lewis to address these deficiencies at the basic as well as the applied levels, with participation by industry and universities. One of these programs was the structures element of the turbine engine Hot Section Technology (HOST) program. The structures element focused on three key technology areas: inelastic constitutive model development, three-dimensional nonlinear structural methods and code development, and experimentation to calibrate and validate the models and codes. These technology areas were selected not only because todays hot section component designs are materially and structurally difficult to analyze with existing analytical tools, but because even greater demands will be placed on the analysis of advanced designs. It is the need for improved engine performance (higher temperatures, lower cooling flows), lower engine weight, and improved engine reliability and durability which will require advanced analytical tools and expanded experimental capabilities.

Because materials used in today's turbine engine hot section components are operating at elevated temperature, time-independent (plastic) and time-dependent (creep and stress relaxation) material behavioral phenomena occur simultaneously, and these phenomena will be exacerbated in future component designs. Classical elastic-plastic theories, where creep and plasticity are uncoupled do not adequately characterize these interactive phenomena. These interactions are captured with inelastic (viscoplastic or unified) constitutive models. Under HOST, several viscoplastic models were developed for high-temperature isotropic and anisotropic nickel-base superalloys used in hot section components. These models were incorporated in several nonlinear three-dimensional structural analysis codes.

The analysis demands placed on hot section component designs result not only from the use of advanced materials and their characterization, but also from the use of new and innovative structural design concepts. There is an obvious need to develop advanced computational methods and codes, with the focus on improved accuracy and efficiency, to predict nonlinear structural response of advanced component designs. Under HOST, improved time-varying thermal-mechanical load models for the entire engine mission cycle from startup to shutdown were developed. The thermal model refinements are consistent with those required by the structural codes, including considerations of mesh-point density, strain concentrations, and thermal gradients. An automated component-specific geometric

modeling capability which will produce three-dimensional finite element models of the hot section components was also developed. Self-adaptive solution strategies were developed and included to facilitate the selection of appropriate elements, mesh sizes, etc. New and improved nonlinear three-dimensional structural analysis codes, including temporal elements with time-dependent properties to account for creep effects in the materials and components, were developed. A data transfer module was developed to automatically transfer temperatures from finite difference and finite element thermal analysis codes to finite element structural analysis codes.

Essential for the confident use of these models and structural analysis codes in the analysis and design of hot section components is their calibration and validation. Under HOST, experimental facilities were upgraded and experiments conducted to calibrate and validate the models and codes developed. Unique uniaxial and multiaxial high-temperature thermomechanical tests were conducted. In addition, unique thermomechanical tests on sections of conventional and advanced combustor liners were conducted in the Structural Component Response rig at NASA Lewis. Extensive, quality databases were generated. Advanced strain and temperature instrumentation was also evaluated.

Table I is a summary of the contracts and grants that were an integral part of the structures element under HOST. The research efforts of the grants and contracts, as well as in-house efforts, are described in the paper along with the most significant of the many accomplishments for each. Figure 1 summarizes the nonlinear structural analysis technologies and activities under HOST.

ISOTROPIC MATERIAL MODELING

Southwest Research Institute Contract

Unified constitutive models were developed for structural analysis of turbine engine hot section components under NASA/HOST contract NAS3-23925, "Constitutive Modeling for Isotropic Materials" (Chan et al., 1986). During this project, two existing models of the unified type were developed for application to isotropic, cast, nickel-base alloys used for air-cooled turbine blades and vanes. The two models are those of Walker (1981), and of Bodner and Partom (1975). Both models were demonstrated to yield good correlation with experimental results for two alloys: PWA alloy B1900+Hf and MAR-M247. The experimental correlations were made with testing under uniaxial and biaxial tensile, creep, relaxation, cyclic, and thermomechanical loading conditions over a range in strain rates and temperatures up to 1100 °C. Also, both models were implemented in the MARC nonlinear finite element computer code with test cases run for a notched round tensile specimen and an airfoil portion of a typical cooled turbine blade.

Typical results of thermomechanical strain cycling of B1900+Hf material are shown in Figs. 2 and 3. In Fig. 2, we show a single specimen cycled to saturation at 538 °C, a temperature increase to 982 °C with saturated loops achieved at that temperature, and a return to 538 °C, all under constant strain range control. Two observations evidence absence of thermal history effect. The high-temperature excursion resulted in no change in the hysteresis loop at 538 °C, and the cyclic stress range associated with a given cyclic strain was the same under this type of nonisothermal history as under strictly isothermal cycling, as shown in Fig. 3. Both types of cycling agree with the Bodner-Partom model prediction which is based on isothermal data only.

A second example is the analysis of an airfoil of a typical cooled turbine blade. Simulations were run in which a classical creep-plasticity model was compared with the Walker and Bodner-Partom models for B1900+Hf material. The airfoil was exercised through three full flight spectra of taxi, take off, climb, cruise, descent, taxi, and shutdown. Computational efficiency with the unified models was as good or better than with a more classical elasticplastic approach. The effective stress versus strain response at the airfoil critical location is compared in Fig. 4 for all three constitutive models. The unified models yield very similar results but substantially different from the classical creep-plasticity model. Unfortunately, no experimental results are available or easily obtainable for this complex problem.

In summary, the program has demonstrated that for the cast nickel-base alloys studied, B1900+Hf and MAR-M247, both isothermal and nonisothermal complex loading histories can be well predicted using the unified constitutive model approach with all necessary material constants derived solely from isothermal test data.

The program has also demonstrated rather conclusively that the unified constitutive model concept is a very powerful tool for predicting material response in hot section components under complex, time-varying, thermomechanical loadings. This confidence is gained from extensive correlations between two existing models and a large base of experimental data covering the range in stress, strain rate, and temperature of interest. The unified constitutive models have also been demonstrated to be computationally efficient when incorporated into a large finite element computer code (MARC).

General Electric Contract

Unified constitutive models were also developed and validated for structural analysis of turbine engine hot section components under NASA/HOST contract NAS3-23927, "Constitutive Modeling for Isotropic Materials," (Ramaswamy, 1986). As part of this effort, several viscoplastic constitutive theories were evaluated against a large uniaxial and multiaxial data base on René 80 material, which is a cast nickel-base alloy used in turbine blade and vane applications. Initially, it was the intent to evaluate only available theories; however, it was found that no available approach was satisfactory in modeling the high temperature time dependent behavior of René 80. Additional considerations in model development included the cyclic softening behavior of René 80, rate independence at lower temperatures, and the development of a new model for static recovery. These considerations were incorporated in a new constitutive model which was implemented into a finite element computer code. The code was developed as a part of the contract specifically for use with unified theories. The code was verified by a reanalysis of the turbine tip durability problem which was part of the pre-HOST activities at General Electric.

Typical of the many results obtained from this effort are the multiaxial thermomechanical comparisons shown in Figs. 5 and 6. Figure 5 shows that the new theory can predict 90° out-of-phase tension/torsion experimental results at elevated temperature with good accuracy. Figure 6 shows a comparison of prediction with experimental data from combined temperature and strain cycling tests. There is reasonably good agreement between predictions and experiment considering the predictions are based only on isothermal data.

The theory was implemented into a new three-dimensional finite element code which uses a 20-noded brick element. The program uses a dynamic time incrementing procedure to minimize cost while guaranteeing an accurate solution. The inelastic rate equations and state variable evolution equations are integrated using a second order Adams-Moulton predictor corrector technique. Piecewise linear load histories are modelled in order to simplify input. Further economics have been achieved by improving the stability of the initial strain method and further reducing the number of equilibrium iterations.

In summary, a new multiaxial constitutive model which can represent the complex nonlinear high temperature behavior of René 80 was developed. The model was extensively verified based on data at several temperatures. The thermomechanical proportional and nonproportional cyclic modeling capabilities of the model were demonstrated. The model was implemented in a three-dimensional structural analysis finite element code and a turbine blade was analyzed.

University of Akron Grant

Many viscoplastic constitutive models for high-temperature structural alloys are based exclusively on uniaxial test data, as previously discussed. Generalization to multiaxial states of stress is made by assuming the stress dependence to be on the second principal invariant (J_2) of the deviatoric stress, frequently called the "effective" stress. Testing other than uniaxial, e.g., shear, biaxial, etc., is generally done in the spirit of verification testing, not as part of the data base of the model. If such a J_2 theory, based on uniaxial testing, is called upon to predict behavior under conditions other than uniaxial, say pure shear, and it does so poorly, nothing is left to adjust in the theory. The exclusive dependence on J_2 must be questioned. For a fully isotropic material whose inelastic deformation behavior is relatively independent of hydrostatic stress, the most general stress dependence is on the two (nonzero) principal invariants of the deviatoric stress, J_2 and J_3. These invariants constitute what is known as an integrity basis for the material.

Under NASA Grant NAG3-379, "A Multiaxial Theory of Viscoplasticity for Isotropic Materials," (Robinson, 1984) a time-dependent description potential function based on constitutive theory with stress dependence on J_2 and J_3 that reduces to a known J_2 theory as a special case was developed. The characterization of viscoplasticity can be made largely on uniaxial testing but the "strength" of the J_3 dependence must be determined by testing other than uniaxial, e.g., pure shear.

Several calculations have been made using forms of the functions in the model and associated material parameters that are typical of ferritic chrome-based and austenitic stainless-steel alloys. Qualitatively similar results can be expected for nickel-based alloys. Figure 7 shows predicted hysteresis loops over a constant strain range ($\Delta\varepsilon$ = 0.6 percent) and strain rate ($\dot{\varepsilon}$ = 0.001/m). The curve labeled "uniaxial" can be thought of as having been carefully fit on the basis of uniaxial data. Predictions of pure shear response are also shown, corresponding to different values of C. A J_2, J_3 theory reduces to a J_2 theory for C = 0. Even after tedious fitting of uniaxial cyclic data, if the shear prediction does not correlate well with shear data, nothing can be done in a J_2 theory short of compromising the uniaxial correlations. The present J_2, J_3 theory allows some flexibility in accurately predicting response other than uniaxial through the parameter C. Note that the hysteresis loop labeled C = 10 indicates a cyclic response that is about 20 percent stronger than the J_2 response (C = 0).

Figure 8 shows predictions of creep response, i.e., behavior under constant stress. Here, the strain-time curve labeled "uniaxial and shear C = 0" represents both the uniaxial response (using the strain scale on the left) and the shear response for a J_2 material (using the strain scale on the right). Each shear response corresponding to a particular value of C is to be measured using the right-hand shear strain scale. In creep, the effect of the J_3 dependence appears to be more pronounced than for strain cycling. Here, for C = 10 the creep strain after 100 hr differs by a factor of 2 from that for the J_2 response (C = 0).

ANISOTROPIC MATERIAL MODELING

University of Connecticut Grant

Nickel-base monocrystal superalloys have been under development by turbine manufacturers for a number of years. Successful attempts have now been made under grant NAG3-512, "Constitutive Modeling of Single Crystal and Directionally Solidified Superalloys," (Walker, and Jordan, 1987) to model the deformation behavior of these materials based on both a macroscopic constitutive model and a micromechanical formulation based on crystallographic slip theory. These models have been programmed as FORTRAN subroutines under contract NAS3-23939 to Pratt and Whitney and included in the MARC nonlinear finite element program. They are currently being used to simulate thermal/mechanical loading conditions expected at the "fatigue critical" locations on a single crystal (PWA 1480) turbine blade. Such analyses form a natural precursor to the application of life prediction methods to gas turbine airfoils.

The difficulty in analyzing the deformation behavior of single crystal materials lies in their anisotropic behavior. Two separate unified viscoplastic constitutive models for monocrystal PWA 1480 have been completely formulated. In one model, the directional properties of the inelastic deformation behavior are achieved by resolving the summed crystallographic slip system stresses and strains onto the global coordinate system. In the other model, the required directional properties are achieved by operating on the global stresses and strains directly with fourth rank anisotropy tensors. The crystallographic slip based model is more accurate and has more physical significance than the macroscopic model, but is more computationally intensive than its macroscopic counterpart.

The material constants in both models can be obtained from uniaxial tests on <001> and <111> oriented uniaxial specimens, or from uniaxial and torsion tests on <001> orientated tubular specimens. Both models achieve good correlation with the experimental data in the <001> and <111> corners of the stereographic triangle, and both models correctly predict the deformation behavior of specimens orientated in the <011> direction. The tension-torsion tests on tubular specimens orientated in the <001> direction were carried out at a temperature of 870 °C (1600 °F) at the University of Connecticut. Further tests at temperatures ranging from room temperature to 1149 °C (2100 °F) have been carried out at Pratt and Whitney under contract NAS3-23939. Good correlations and predictions are uniformly achieved at temperatures above 649 °C (1200 °F), but further work appears to be necessary to correctly model the deformation behavior of PWA 1480 monocrystal material below 649 °C (1200 °F).

University of Cincinnati Grant

Nickel base single crystal superalloys have attracted considerable interest for use in gas turbine jet engine because of their superior high temperature properties. In polycrystalline turbine parts, rupture is usually due to crack propagation originating at the grain boundaries. Since single crystal alloys have no grain boundaries, use of the alloy has significant advantages for increased strength and longer life.

Under grant NAG3-511, "Anisotropic Constitutive Modeling for Nickel-Base Single Crystal Alloy René N4," an anisotropic constitutive model was developed based on a crystallographic approach. The current equations modified a previous model proposed by Dame and Stouffer (1986) where a Bodner-Partom equation with only the drag stress was used to model the local inelastic response in each slip system. Their model was considered successful for predicting both the orientation dependence and tension/compression asymmetry for tensile and creep histories for single crystal alloy René N4 at 760 °C (1400 °F). However, certain properties including fatigue were not satisfactorily modeled. A back stress state variable was incorporated into the local slip flow equation based on the observed experimental observations. Model predictability was improved especially for mechanical properties such as inelasticity and fatigue loops.

Figures 9 and 10 are typical of the numerous results obtained from this effort. Experimental data and predicted responses of tensile and cyclic conditions for different specimen orientations are compared. Shown in Fig. 9 are the experimental data in [100] and [111] orientations which were used to determine material constants. The response in [110] orientation is the predicted result. The model predicted very well the elastic moduli, hardening characteristics (the knee of the curves) and the saturated values. In Fig. 10, comparisons show the model predicts very well the cyclic tension/compression asymmetry, hardening characteristics and rate effect for the [100] orientation. The prediction of the hystersis loop was based solely on saturated constants determined from tensile tests.

University of Akron Grant

Structural alloys used in high-temperature applications exhibit complex thermomechanical behavior that is time-dependent and hereditary. Recent attention is being focused on metal-matrix composite materials for aerospace applications that, at high temperature, exhibit all the complexities of conventional alloys (e.g., creep, relaxation, recovery, rate sensitivity) and, in addition, exhibit further complexities because of their strong anisotropy.

Under grant NAG3-379, "A Continuum Deformation Theory for Metal-Matrix Composites at High Temperature," (Robinson et al., 1986) a continuum theory was developed for representing the high-temperature, time-dependent, hereditary deformation behavior of metallic composites that can be idealized as pseudohomogeneous continua with locally definable directional characteristics. Homogenization of textured materials (molecular, granular, fibrous) and applicability of continuum mechanics in structural applications depends on characteristic body dimensions, the severity of gradients (stress, temperature, etc.) in the structure and on the relative size of the internal structure (cell size) of the material. Examination reveals that the appropriate conditions are met in a significantly large class of anticipated aerospace applications of metallic composites to justify research into the formulation of continuum-based theories.

The starting point for the theoretical development is the assumed existence of a dissipation potential function Ω for a composite material; that is a two constituent (fiber/matrix), pseudohomogeneous material.

The potential function is of the form

$$\Omega = \Omega(\sigma_{ij}, \alpha_{ij}, d_i d_j, T) \qquad (1)$$

in which σ_{ij} denotes the components of (Cauchy) stress, α_{ij} the components of a tensorial internal state variable (internal stress), $d_i d_j$ the components of a directional tensor, and T the temperature. The symmetric tensor $d_i d_j$ is formed by a self product of the unit vector d_i denoting the local fiber direction. Account can be taken of more than a single family of fibers inherent to the continuum element.

The present theory has been implemented into the commercial finite element code MARC. Several trial calculations have been made under uniaxial conditions using material functions and parameters that approximate a tungsten/copper composite material. A transversely isotropic continuum elasticity theory has been used in conjunction with the present viscoplastic theory. The results of the calculations show the expected responses of rate-dependent plasticity, creep, and relaxation as well as appropriate anisotropic features. Predictions of relaxation and hysteresis loops for different fiber orientation angles on a tungsten/copper like material are shown in Figs. 11 and 12.

COMPUTATIONAL METHODS AND CODE DEVELOPMENT

General Electric Contract

It has become apparent in recent years that there is a serious problem of interfacing the output temperatures and temperature gradients from either the heat transfer codes or engine tests with the input to the stress analysis codes. With the growth in computer postprocessors, the analysis of hot section components using hundreds and even thousands of nodes in the heat transfer and stress models has become economical and routine. This has exacerbated the problem of manual transfer of output three-dimensional temperatures from heat transfer codes to stress analysis input to where the engineering effort required is comparable to that required for the remainder of the analysis. Furthermore, a considerable amount of approximation has been introduced in an effort to accelerate the process. This tends to introduce errors into the temperature data which negates the improved accuracy in the temperature distribution achieved through use of a fine mesh. There is, then, a strong need for an automatic thermal interface module. A module was developed under contract NAS3-23272, "Burner Liner Thermal/Structural Load Modeling," (Maffeo, 1984).

The overall objectives of this thermal/structural transfer module were that it handle independent mesh configurations, finite difference and finite element heat transfer codes, perform the transfer in an accurate and efficient fashion and the total system be flexible for future applications. Key features of the code developed include: independent heat transfer and stress model meshes, accurate transfer of thermal data, computationally efficient transfer, user friendly program, flexible system, internal coordinate transformations, automated exterior surfacing techniques and geometrical and temporal windowing capability.

A schematic of the TRansfer ANalysis Code (TRANCITS) is shown in Fig. 13. The module can process heat transfer results directly from the MARC (finite

element) and SINDA (finite difference) programs and will output temperature information in the forms required for MARC and NASTRAN. The input and output routines in the module are very flexible and could easily be modified through a neutral file to except data from other heat transfer codes and format data to other stress analysis codes.

This thermal load transfer module has been shown to efficiently and accurately transfer thermal data from dissimilar heat transfer meshes to stress meshes. The fundamental part of the code, the three-dimensional search, interpolation and surfacing routines, have much more potential. They form an outstanding foundation for automatic construction of embedded meshes, local element mesh refinement, and the transfer of other mechanical type loading.

General Electric Contract

The overall objective of this program was to develop and verify a series of interdisciplinary modeling and analysis techniques specialized to address hot section components. These techniques incorporate data as well as theoretical methods from many diverse areas including cycle and performance analysis, heat transfer analysis, linear and nonlinear stress analysis, and mission analysis. Building on the proven techniques already available in these fields, the new methods developed through this contract were integrated into a system which provides an accurate, efficient, and unified approach to analyzing hot section structures. The methods and codes developed under this contract, NAS3-23687, "Component-Specific Modeling," (McKnight, 1985) predict temperatures, deformation, stress and strain histories throughout a complete flight mission.

Five basic modules were developed and then linked together with an executive module. They are:

(1) The Thermodynamic Engine Model (TDEM) which is the subsystem of computer software. It translates a list of mission flight points and delta times into time profiles of major engine performance parameters. Its present data base contains CF6-50C2 engine performance data. In order to adapt this system to a different engine requires only the restocking of this data base with the appropriate engine performance data.

(2) The Thermodynamic Loads Model (TDLM) which is the subsystem of computer software which works with the output of the TDEM to produce the mission cycle loading on the individual hot section components. There are separate segments for the combustor, the turbine blade, and the turbine vane. These segments translate the major engine performance parameter profiles from the TDEM into profiles of the local thermodynamic loads (pressures, temperatures, rpm) for each component. The formulas which perform this mapping in the TDLM models were developed for the specific engine components. To adapt these models to a different engine would require evaluating these formulas for their simulation capability and making any necessary changes.

(3) The Component Specific Structural Modeling which is the heart of the geometric modeling and mesh generation using the recipe concept. A generic geometry pattern is determined for each component. A recipe is developed for this basic geometry in terms of point coordinates, lengths, thicknesses, angles, and radii. These recipe parameters are encoded in computer software as variable input parameters. A set of default numerical values are stored for these parameters. The user need only input values for those parameters which are to have different values. These recipe parameters then uniquely define a generic component with the defined dimensions. The software logic then works with these parameters to develop a finite element model of this geometry consisting of 20-noded isoparametric elements. The user specifies the number and distribution of these elements through input control parameters. Figure 14 shows the generic geometry and recipe for a combustor liner panel.

(4) The subsystem which performs the three-dimensional nonlinear finite element analysis of the hot section component model and was developed under the NASA HOST contract NAS3-23698, "three-dimensional Inelastic Analysis Methods for Hot Section Structures." This software performs incremental nonlinear finite element analysis of complex three-dimensional structures under cyclic thermomechanical loading with temperature dependent material properties and material response behavior. The nonlinear analysis considers both time-independent and time-dependent material behavior. Among the constitutive models available is the Haisler-Allen classical model which performs plasticity analysis with isotropic material response, kinematic material response, or a combination of isotropic and kinematic material response. This is combined with a classical creep analysis formulation. A major advance in the ability to perform time-dependent analyses is a dynamic time incrementing strategy incorporated in this software.

(5) The COSMO system which consists of an executive module which controls the TDEM, TDLM, the geometric modeler, the structural analysis code, the file structure/data base, and certain ancillary modules. The ancillary modules consist of a band width optimizer module, a deck generation module, a remeshing/mesh refinement module and a postprocessing module. The executive directs the running of each module, controls the flow of data among modules and contains the selfadaptive control logic. Figure 15 is a flow chart of the COSMO system showing data flow and the action positions of the adaptive controls. The modular design of the system allows each subsystem to be viewed as a plug-in module. They can be abstracted and run alone or replaced with alternate systems.

The ideas, techniques, and computer software developed in the Component Specific Modeling program have proven to be extremely valuable in advancing the productivity and design-analysis capability for hot section structures.

General Electric Contract

Under NASA contract NAS3-23698, "Three-Dimensional Inelastic Analysis Methods for Hot Section Components," (McKnight et al., 1986), a series of three-dimensional inelastic structural analysis computer codes were developed and delivered to NASA Lewis. The objective of this program was to develop analytical methods capable of evaluating the cyclic time-dependent inelasticity which occurs in hot section engine components. Because of the large excursions in temperature associated with hot section engine components, the techniques developed must be able to accommodate large variations in material behavior including plasticity and creep. To meet this objective, General Electric developed a matrix consisting of three constitutive models and three element formulations. A separate program for each combination of constitutive model-element model was written, making a total of

nine programs. Each program was given a stand alone capability of performing cyclic nonlinear analysis.

The three constitutive models are in three distinct forms: a simplified theory (simple model), a classical theory, and a unified theory. In an inelastic analysis, the simplified theory uses a bilinear stress-strain curve to determine the plastic strain and a power law equation to obtain the creep strain. The second model is the classical theory of Haisler and Allen. The third model is the unified model of Bodner and Partom. All of the models were programmed for a linear variation of loads and temperatures with the material properties being temperature dependent.

The three element formulations used are an 8-node isoparametric shell element, a 9-node shell element, and a 20-node isoparametric solid element. The 8-node element uses serendipity shape functions for interpolation and Gaussian quadrature for numerical integration. Lagrange shape functions are used in the 9-node element. For numerical integration, the 9-node element uses Simpson's rule. The 20-node solid element uses Gaussian quadrature for integration.

For the linear analysis of structures, the nine codes use a blocked-column skyline, out-of-core equation solver. To analyze structures with nonlinear material behavior, the codes use an initial stress iterative scheme. Aitken's acceleration scheme was incorporated into the codes to increase the convergence rate of the iteration scheme.

The ability to model piecewise linear load histories was written into the codes. Since the inelastic strain rate can change dramatically during a linear load history, a dynamic time-incrementing procedure was included. The maximum inelastic strain increment, maximum stress increment, and the maximum rate of change of the inelastic strain rate are the criteria that control the size of the time step. The minimum time step calculated from the three criteria is the value that is used.

In dynamic analysis, the eigenvectors and eigenvalues can be extracted using either the determinant search technique or the subspace iteration method. These methods are only included with those finite-element codes containing the 8-node shell element.

Pratt and Whitney Aircraft Contract

The objective of the work done under contract NAS3-23697, "Three-dimensional Inelastic Analysis Methods for Hot Section Components," (Nakazawa, 1987; Wilson, and Banerjee, 1986) was to produce three new computer codes to permit accurate and efficient three-dimensional inelastic analysis of combustor liners, turbine blades, and turbine vanes. The three codes developed are called MOMM (Mechanics of Materials Model), MHOST (MARC-HOST) and BEST (Boundary Element Stress Technology). These codes embody a progression of mathematical models for increasingly comprehensive representation of the geometrical features, loading conditions, and forms of nonlinear material response that distinguish the three groups of hot section components.

Software in the form of stand-alone codes was developed by Pratt and Whitney Aircraft (PWA) with assistance from three subcontractors: MARC Analysis Research Corporation (MARC), United Technology Research Center (UTRC), and the State University of New York at Buffalo (SUNY-B).

Three increasingly sophisticated constitutive models were implemented in MOMM, MHOST, and BEST to account for inelastic material behavior (plasticity, creep) in the elevated temperature regime. The simplified model assumes a bilinear approximation of stress-strain response and glosses over the complications associated with strain rate effects, etc. The state-of-the-art model partitions time-independent plasticity and time-dependent creep in the conventional way, invoking the von Mises yield criterion and standard (isotropic, kinematic, combined) hardening rules for the former, and a power law for the latter. Walker's viscoplasticity theory which accounts for the interaction between creep/relaxation and plasticity that occurs under cyclic loading conditions, has been adopted as the advanced constitutive model.

MOMM - This is a stiffness method finite element code that utilizes one-, two- and three-dimensional arrays of beam elements to simulate hot section component behavior. Despite limitations of such beam model representations, the code will be useful during early phases of component design as a fast, easy to use, computationally efficient tool. All of the structural analysis types (static, buckling, vibration, dynamics), as well as the three constitutive models mentioned above, are provided by MOMM. Capabilities of the code have been tested for a variety of simple problem discretizations.

MHOST - This code employs both shell and solid (brick) elements in a mixed method framework to provide comprehensive capabilities for investigating local (stress/strain) and global (vibration, buckling) behavior of hot section components. Attention was given to the development of solution algorithms, integration algorithms for stiffness, strain recovery and residual terms, and modeling methods that permit accurate representations of thermal effects on structural loading and material properties, as well as geometrical discontinuities.

The three constitutive models implemented are the secant elasticity model, von Mise's plasticity model, and Walker's creep plasticity model. Temperature dependency and anisotropy can be obtained through user subroutines in MHOST. Nonlinear transient analysis and eigenvalue extraction for buckling and modal analyses are some of the other important features in the program. The improved algorithm models and finite elements implemented in the code significantly reduced CPU (Central Processing Units) time requirements for three-dimensional analyses.

To test the validity of the MHOST finite-element code, considerable efforts were made in applying the code in different cases with results compared to theoretical predictions or numerical values generated by other codes. For example, the code was used in-house to analyze a General Electric CF/6-50 engine blade and rotor model with data generated by a computational structural mechanics simulator system. The simulator system provided data, such as pressure and temperature distribution, centrifugal force, and time duration, at various stages of flight. Figure 16 shows the variation of the radical displacement of the leading edge tip in the static condition during the entire flight without consideration of the centrifugal force effect.

BEST3D - This is a general purpose three-dimensional structural analysis program utilizing the boundary element method. The method has been implemented for very general three-dimensional geometries, and for elastic, inelastic and dynamic stress analysis. Although the feasibility of many of the capabilities provided has been demonstrated in a number of individual prior research efforts, the present code is the first in which they have been made available for large scale problems in a single code. In addition, important basic advances have been made in a number of areas, including the development and implementation of a variable stiffness plasticity algorithm, the incorporation of an embedded time algorithm for elastodynamics and the extensive application of particular

solutions within the boundary element method. Major features presently available in the BEST3D code include: very general geometry definition, including the use of double curved isoparametric surface elements and volume cells, with provision of full substructuring capability; general capability for the definition of complex, time-dependent boundary conditions; capability for nonlinear analysis using a variety of algorithms, solution procedures and constitutive models; and a very complete elastodynamic capability including provision for free vibration, forced response and transient analysis.

The BEST3D code was validated by comparing predictions from BEST3D with those from theoretical and/or numerical predictions and some experimental data. For example, results from a benchmark notch test program were used. Finite element and boundary element meshes for one-quarter of a specimen gage section are shown in Fig. 17. Measurements of notch root stress-strain behavior for initial uploadings were compared with predictions (Fig. 18). Simulation of first-cycle notch root behavior with BEST3D was proven to be quite accurate.

EXPERIMENTAL FACILITIES AND DATA

Oak Ridge National Laboratory Interagency Agreement

An experimental effort was undertaken under Interagency Agreement Number 40-1447-84 and U.S. Department of Energy contract DE-AC05-840R 21400 with Martin Marietta Energy Systems Inc., "Determination of Surface of Constant Inelastic Strain Rate at Elevated Temperature," (Battiste, and Ball, 1986). Special exploratory multiaxial deformation tests on tubular specimens of type 316 stainless steel at 649 °C (1200 °F) were conducted to investigate time-dependent material behavior.

In classical plasticity the concept of yield surfaces in multiaxial stress space plays a central role, not only in the definition of initial yielding but in determining subsequent plastic flow. At high temperatures the deformation behavior of structural alloys is strongly time dependent. Consequently, the significance of yield surfaces breaks down, and it has been proposed that in their place the concept of surfaces of constant inelastic strain rate (SCISR) might be utilized. Such surfaces, called SCISRs, can be shown to have a potential nature and thus constitute the basis of a rational multiaxial viscoplastic constitutive theory.

A surface of constant inelastic strain rate was determined by loading the specimen at a constant effective stress rate in the two-dimensional axial/torsional stress state in various directions until a predetermined inelastic effective strain rate was reached. After each probe, the stress was returned to the initial starting point; thus a locus of points (surface of constant inelastic strain rate) was established.

Two types of tests were conducted. One test specimen was subjected to a time-independent torsional shear strain test history, and surfaces of constant inelastic strain rate (SCISRs) in an axial/torsional stress space were measured at various predetermined points during the test. A second specimen was subjected to a 14-week time-dependent (creep-recovery-creep periods) torsional shear stress histogram. SCISRs determinations were made at 17 points during the test. The tests were conducted in a high-temperature, computer-controlled axial/torsional test facility using an Oak Ridge National Laboratory developed high-temperature multiaxial extensometer.

A key result of this testing effort was that surfaces of constant inelastic strain rate exist and can be determined or measured at an elevated temperature, 650 °C. This is shown in Fig. 19. The conclusion is validated or deduced by the execution of the test programs and by the consistency of the surface results, especially the repeated surfaces. To our knowledge, this is the first successful determination of high-temperature surfaces of constant inelastic strain rate.

Although conclusions regarding the effect of these SCISRs data on different theories will be left to the constitutive equation developers, several results can be stated. First, the surfaces did not move or change shape in the axial/torsional stress state by any significant amount. Second, a deduction that plastic deformations have a larger effect than creep deformations can be stated. Third, SCISRs determined immediately after large plastic deformation show more inconsistent results than SCISRs which have not undergone immediate prior plastic deformations. Last, the extensometer system and software control system performed extremely well in a difficult application.

In-house Lewis Research Center Experimental Facilities and Data

Uniaxial Test Systems. Under HOST, recent expansion of the uniaxial testing capability of the fatigue and structures laboratory included the addition of four new test systems (Bartolotta, and McGaw, 1987). One of these systems is shown in Fig. 20. The load rating for two of the new systems is ±9072 kg (±20 000 lb), and the other two at ±22 680 kg (±50 000 lb). Each system is equipped with a state-of-the-art digital controller. The digital controllers have the ability to complete a smooth control mode transfer, which is accomplished either manually or electronically. This feature will make it possible to conduct some of the more complex tests that have been defined by the constitutive model developers at NASA Lewis and elsewhere. Specimen heat is provided by 5 kW radio frequency induction heaters. Axial strains are measured using an axial extensometer. To study the effects of the environment on creep-fatigue behavior, the two smaller load capacity test systems are equipped with environmental chambers capable of providing a vacuum and/or an inert environment. The environmental chamber is able to sustain a vacuum of 2.67×10^{-4} Pa (2×10^{-6} torr) with a specimen temperature of 1093 °C (2000 °F). All systems include water-cooled hydraulic grips for simple specimen installation. By the means of exchanging two collets these grips can be adapted to handle either flat bar, smooth shank, or threaded-end specimens. Each uniaxial system has its own minicomputer for experimental control and data acquisition. Preliminary software has been developed by the experimentalists to conduct tests as simple as a low cycle fatigue test, and as complicated as thermomechanical tests.

Biaxial Test Systems. In many life and material behavior models, multiaxial representations are formulated by modifying uniaxial criteria. Unfortunately, this method does not always achieve the accuracy needed to meet design goals of hot section components. In response to this need for better life and material behavior predictions under complex states of stress and strain, a multiaxial testing capability is being developed. As an evolutionary step from a uniaxial test capability, a decision was made to begin with biaxial (axial-torsion) test systems (Fig. 21) and

eventually progress to triaxial systems through the use of internal pressure. Under HOST, three new biaxial test systems were added to the laboratory (Bartolotta, and McGaw, 1987).

The load frames for each test system are rated for loads of ±22 948 kg (±50 000 lb) axial and ±2824 N-m (±25 000 in.-lb) torsional. Electronics for these systems consist of two servocontrollers, two data display units, function generators, and an oscilloscope. The two servocontrollers allow for both independent and combined control of axial and torsional loading. Each servocontroller can control specimen loading in one of three modes: load, strain or stroke for axial loading and torque, torsional strain or angular displacement for torsional loading. Data display units are used to monitor analog data signals, and provide an important interface between the test system and the computer system. These units can be programmed to perform a variety of signal processing operations.

The heating system for each biaxial test system consists of an audio frequency induction generator, an induction coil fixture, and a PID controller for closed-loop temperature control. Each generator has a power output of 50 kW at an operating frequency of 9.6 kHz. Audio frequency generators were chosen because of their ability to operate with minimal electrical interference to instrumentation signals.

Each axial-torsional test system is interfaced with its own minicomputer. These minicomputers, along with the data display units, are used for experimental control and data acquisition. Preliminary software is being used to conduct simple tests, while more complicated test programs are still in their developmental stages.

A thin-walled tube was chosen as the basic specimen geometry. This type of geometry has the following advantages: (a) easy decomposition of axial-torsional components of stress and strain, (b) at high temperatures thermal gradients across the diameter are minimal, and (c) for thermomechanical testing, cooling rates are higher.

Uniaxial Experimental Results. Extensive databases for several materials have been generated under the grants and contracts previously discussed. In the Lewis Fatigue and Structures Laboratory, a uniaxial database on Hastelloy-X, a nickel-base superalloy used in hot section component applications, was generated (Bartolotta, 1985; Ellis et al., 1986; Bartolotta, and Ellis, 1987). These data are being used in the development and calibration of constitutive models. In addition, some of the data generated was used to address a number of questions regarding the validity of methods adopted in characterizing the constitutive models for particular high-temperature materials. One area of concern is that the majority of experimental data available for this purpose are determined under isothermal conditions. This is in contrast to service conditions which almost always involve some form of thermal cycling. The obvious question arises as to whether a constitutive model characterized using an isothermal data base can adequately predict material response under thermomechanical conditions. Described here is an example of results of the most recent isothermal and thermomechanical experiments conducted on Hastelloy-X to address this concern.

Results obtained from two uniaxial isothermal (205 and 425 °C) and one out-of-phase uniaxial thermomechanical (200 to 400 °C) experiments are presented in Fig. 22. The thermomechanical test was conducted in such a way that the mechanical strain range and mechanical strain rate were similar to what was used for the isothermal experiments. Because of the temperature response limitations of the experiment itself, it should be noted that at the tensile peaks of each thermomechanical cycle, the temperature undershot its lower bound by -5 °C (195 °C instead of 200 °C).

From Fig. 22 it can be observed that at the tenth cycle of the isothermal tests the stress - inelastic strain responses are similar. As for the thermomechanical test, the stress - inelastic strain response is slightly different compared to the isothermal data. This is probably due to the difference in mechanical strain range caused by the temperature overshoot. As can be seen, the stress - inelastic strain response for the thermomechanical experiments seems to follow more closely that of the lower temperature isothermal test. As cycling continues, the thermomechanical material response seems to start following that of the higher temperature isothermal experiment. This observation was also observed in another thermomechanical experiment (400 to 600 °C), which suggests that this trend is a general material hardening characteristic, but further investigation will have to be conducted before this can be confirmed.

Preliminary inelastic strain comparisons between isothermal and thermomechanical experimental data have proven useful in developing a better understanding of thermomechanical material response for Hastelloy-X. From these types of comparisons it appears that general thermomechanical material behavior can be extracted from isothermal experimental data, but information concerning changes in material strain hardening behavior must come from thermomechanical test data.

Tests on Haynes 188, a cobalt-based superalloy used in hot section component applications were also conducted in the laboratory (Ellis et al., 1987). An example of the test results obtained is presented. In this example we are concerned with determining the stress levels or "thresholds" at which creep deformations first become significant in Haynes 188 over a temperature range of interest. A second series of experiments was conducted to establish whether the thresholds determined under monotonic conditions also apply in the case of thermomechanical loading.

As shown in Table II, the threshold experiments showed the expected result that early creep response is strongly temperature dependent. It can be seen that at 649 °C, stress levels must exceed 207 MPa (30 ksi) before creep strains become significant during the 1.5 hr hold periods. At temperatures of 760 and 871 °C, the corresponding values of stress are 75.9 MPa (11 ksi) and 27.6 MPa (4 ksi), respectively. One important point to be noted about this result is that it would not have been predicted by inspection of handbook data. This is because material handbooks provide little or no information regarding the early stages of creep. It follows that problems can arise if decisions regarding the need for inelastic analysis are based on casual inspection of handbook data. The present study clearly indicated that some form of inelastic analysis is necessary for components operating at temperatures as high as 871 °C if stress levels are expected to exceed 27.6 MPa (4 ksi).

Turning to the results of the thermomechanical experiments on Haynes 188, ratchetting behavior can be observed in the data shown in Fig. 23 for a mean stress of 42.5 MPa (6.17 ksi). In this case, the creep strain accumulated during cycle (1) was about 100 με. On subsequent cycles, the creep occurring per

cycle was 50 με or less and the data exhibited considerable scatter. The reason for the scatter is the electrical noise which complicated interpretation of the 42.5 MPa (6.17 ksi) mean stress data.

The material exhibited creep ratchetting during simulated service cycles. This result was not predicted by analysis using current constitutive models for Haynes 188.

Lewis Annular Combustor Liner Test Facility Structural Component Response Rig

Segments, or cylindrical sections of gas turbine engine combustor liners were radiantly heated in the Structural Component Response rig shown in Fig. 24. Quartz lamps were used to cyclically heat the 20-in (0.5 m) diameter test liners. This resulted in axial and circumferential temperature variations as well as through-the-thickness temperature gradients in the test liner similar to those of in-service liners, and thus similar thermally induced stresses and strains. A typical engine mission cycle (take-off, cruise, landing, and taxi) of 3 to 4 hr was simulated in 2 to 3 min. The simulated cyclic temperatures and temperature gradients were felt to be adequate to capture the time-independent and time-dependent interactions resulting in deformation as well as the low-cycle thermal fatigue phenomena of in-service liners. The primary purpose of the rig was to generate large quality thermomechanical databases on combustor liners (Thompson, and Tong, 1986).

The test program was a cooperative effort with Pratt and Whitney Aircraft (PWA), a division of United Technologies Research, East Hartford, Connecticut. PWA supplied the test rig, which included the quartz lamp heating system and several test liners. Lewis provided the test facility and had the responsibilities from integrating the test rig into the test facility up to and including conducting the tests and acquiring the data. Lewis and PWA personnel developed automated computer control strategies, data acquisition systems, and methods for efficient data reduction and analysis.

The quartz lamp heating system consists of 112-6-kVA lamps configured circumferentially in 16 sectors, each having 7 lamps. This system, in addition to drawing up to 672 kVA of 480-V power, requires 3.5 lb/sec of ambient temperature air at 5 psig, 1.5 lb/sec ambient temperature air at 1 psig and 80 gal/min of specially treated water for cooling the rig.

A natural-gas and air mixture is burned in a combustor can upstream of the test section to provide preheated cooling air to the test liner. Cooling air temperatures are controllable from 205 to 316 °C (400 to 600 °F) by varying the fuel/air mixture ratio. The test liner cooling airflow rate is variable from about 4.0 to 7.5 lb/sec at 35 psig. Both the cooling-air temperature and flow rate can be varied to obtain the desired cyclic temperatures on the test liner.

The annular rig has six 5-in. diameter quartz window viewports, three of which are spaced at 120° apart and are used to view the middle section of the test liner. The other three, also spaced at 120° apart, are used to view the upstream portion of the liner and its attachment piece. These windows are rotated 45° from the liner windows. The quartz windows are air and water cooled. Through these windows television, infrared, and high resolution cameras are used to monitor liner condition, temperature, and deformation, respectively.

A microprocessor with a dual-loop programmable controller is used to control the power to the lamps. A specified power-time history is programmed into the microprocessor, and the cooling air temperature and flow rate are appropriately set so that when combined, the desired thermal cycle is imposed on a test liner.

Thermocouples and an infrared thermovision system are used to obtain surface temperatures on the test liner. There are provisions for having a total of 140 thermocouples on the test liner. Both thermocouple and thermal image data are obtained on the cool side of the test specimen. Only thermocouple data are obtained on the hot side (facing the quartz lamps) of the test liner. The thermocouple data provide temperatures at discrete points, while the infrared system provides detailed maps of cool-side thermal information.

The thermal images obtained from the infrared camera are stored on a VHS tape recorder, with the clock time superimposed on each image. Images of the test specimen of from about 4 to about 1 in. in diameter (for finer resolution of temperatures) can be obtained with the zooming capability of the infrared system. Thirty thermal images are captured on tape every second. A computer system is then used to process, reduce, enhance, and analyze the transient temperature information. These data are also compared with the thermocouple data. Thermocouple data are used in the calibration of the infrared system.

During a test run both the facilities data (pressures flows, power, etc.) and the research data (primarily temperature) are acquired for each thermal cycle using the ESCORT II data acquisition system at Lewis. These data are stored automatically once every second on a mainframe computer for later reduction and analysis.

Liner Tests and Results

Two combustor liner segments were tested in the Structural Component Response Rig. First, a conventional liner of sheet metal seam-welded louver construction from Hastelloy-X material (Fig. 25) was tested. Second, an advanced paneled liner (Fig. 25) was tested.

A large, quality (thermocouple (96 TC's) and IR) temperature database was obtained on the conventional liner. Some typical thermocouple data are shown in Fig. 26. The corresponding power history for the thermal cycle is shown in Fig. 27. Figure 26 shows the transient temperature response at three locations on louver 5. The temperature measurements are used in the heat transfer/structural analysis of the liner.

The liner was thermally cycled for almost 1800 cycles. Between 1500 and 1600 cycles an axial crack about 0.2 in. in length developed in the liner. This crack occurred at a hot spot which developed because of closure of several cooling holes. There was no thermocouple right at the hot spot, but surrounding TC's indicated the maximum temperature was at least 937 °C (1720 °F) and could have been over 976 °C (1890 °F).

A composite photograph of the liner after 1782 cycles is shown in Fig. 28. This shows that most of the distortion occurred in louvers 4 to 7, particularly in the bottom (180°) and left (270°) views. The top (0°) and right (90°) views show less distortion.

The test program was terminated after 1782 cycles because the distortion of the louvers became severe enough to contact the frame of one of the quartz lamp banks. Measurements of the crack from the initial observation at 1600 to 1728 cycles indicated 2 percent increase in length.

The distortion of the louvers is typical of liners run in service. The distortion shows some symmetry to the heat pattern of the lamps in that the peaks

of distortion are at the longitudinal center of a lamp bank where the maximum heat flux occurred. It should be noted that a distortion peak was not formed at every bank of lamps.

Similarly, a large quality data base on the advanced combustor liner is being obtained. This liner, consisting of small panels and an outer support shell to which the panels are attached, is instrumented with 125 thermocouples, 73 on the hot side of the panels and 52 on the support shell. A grid system of lines of temperature-sensitive paints was applied to over half of the panels in the liner to increase the area in which we could observe temperature changes. An infrared camera system is being used to obtain temperature maps of a portion of the outer shell of the liner through a quartz viewing window. Over the same field of view, high-resolution photographs of the outer shell are also being taken to determine the total strain during cycling.

Figure 29 is representative of the data obtained on the advanced liner. It is an isometric plot of the thermocouple temperature measurements of the hot side of the liner panels (which shows the cylindrical liner as if it were cut upon and flattened out) and shows a maximum temperature of 760 °C (1400 °F) at the maximum quartz lamp power (cruise condition). A similar plot of the outer shell shows the maximum temperature to be about 316 °C (600 °F). These temperatures were obtained for a heat flux equivalent to that applied to the conventional liner. Transient data are also being obtained. The thermal paint did not indicate a maximum temperature of more than about 649 °C (1200 °F). The infrared data and the high-resolution photographs are being reduced and analyzed.

After 1500 thermal cycles the advanced liner is operating at much lower temperatures than the conventional liner (about 205 °C (400 °F) lower) for the same heat flux. At the lower temperature and low thermal gradients, little distortion to the panels has been observed. Based on the test results and analyses, the operating conditions are not severe enough to distort or damage the advanced liner.

Thermal/Structural/Life Analyses of the Test Liners

The liner surface temperature measurements obtained from the thermocouples and the infrared thermovision system were used to obtain the film coefficients on the cool and hot surfaces. Based on these coefficients, a heat transfer analysis of each liner was performed using MARC, a general purpose nonlinear finite-element heat-transfer and structural-analysis program.

Eight-node three-dimensional solid elements were used to construct the liner heat transfer models. The conventional liner model had 546 elements and 1274 nodes, and the advanced liner model had 536 elements and 1117 nodes. Comparisons between predicted and measured transient temperatures showed good agreement.

The temperature (or thermal loads) are input to the structural analysis program. The MARC program was used to perform the structural analysis. The stress models were identical to the heat transfer models.

The Walker and Bodner viscoplastic models, which were described earlier, were used in the structural analysis. Representative results are the hysteresis loops shown in Fig. 30 for three locations on the conventional liner. Similarly, Fig. 31 is representative of a stress plot of a symmetrically heated panel.

Based on the nonlinear structural analyses of the two liners, it was determined that the critical stress-strain location in the advanced liner was at the retention loop. For the conventional liner, the critical location was at the seam weld.

Based on the stress-strain and temperature at the critical locations, cyclic life of the two liners was assessed. The results are summarized and compared in Table II. The estimated life of the conventional liner (400 to 1000 cycles) is based on limited cyclic life data. Tests showed liner cracking at the seam weld after 1500 cycles. The advanced liner will have a much longer life than the conventional liner because it has a lower average temperature (about 215 °C (440 °F)) and no structural constraint in the circumferential direction. After 1500 cycles the advanced liner shows little distortion and no cracking. The predicted life is greater than 10^6 cycles. These comparisons show there is good agreement between predicted life and measured life.

CONCLUSIONS

The broad scope of structural analysis activities carried out under the HOST project, by the combined efforts of industry, government and universities has resulted in numerous significant accomplishments and, in some cases, major breakthroughs in the nonlinear three-dimensional structural analyses of turbine engine hot section components. The major accomplishments in the three areas of technology addressed synergistically, namely, inelastic constitutive model development, nonlinear three-dimensional structural analysis methods and code development, and experimentation to calibrate and validate the codes are summarized below:

(1) New types of multiaxial viscoplastic constitutive models for high-temperature isotropic and anisotropic (single crystal) superalloys, and metal matrix composites have been developed, calibrated, and validated.

(2) New and improved nonlinear structural analysis methods and codes, in which the viscoplastic constitutive models were incorporated have been developed and, to some extent, validated.

(3) Extensive quality databases, including uniaxial and multiaxial thermomechanical data, were generated for René N4, René 80, Hastelloy-X, MAR M247, B-1900+Hf, PWA1480 and Haynes 188 materials for the purpose of calibrating and validating the constitutive models.

(4) Extensive quality databases have been generated for conventional and advanced combustor liner segments and compared with detailed thermal/structural analyses of these liners using many of the analytical tools developed under HOST.

(5) Advanced instrumentation to measure temperature, displacement and strain have been evaluated.

(6) High temperature laboratories and facilities at universities, other governmental agencies, and industry have been modified and upgraded, and at NASA Lewis, a unique high-temperature fatigue and structures research laboratory has been implemented.

(7) At NASA Lewis, a high-temperature structural component response research facility for testing large diameter combustor liner segments has been implemented.

While the structural analysis capabilities and accomplishments described in this paper are a good beginning, there is much room for improvement. It is expected that these capabilities and future improvements will grow rapidly in their engineering applications and have a major impact and payoff in the analysis and design of the next generation aeronautic and aerospace propulsion systems.

REFERENCES

Chan, K.S., Lindholm, U.S., Bodner, S.R., Hill, J.T., Weber, R.M., and Meyer, T.G., 1986, NASA CR-17922.

Walker, K.P., 1981, "Research and Development Program for Non-Linear Structural Modeling With Advanced Time-Temperature Dependent Constitutive Relationships," NASA CR-165533.

Bodner, S.R. and Partom, Y., 1975, "Constitutive Equations for Elastic-Viscoplastic Strain-Hardening Materials," Journal of Applied Mechanics, Vol. 42, No. 2, pp. 385-389.

Ramaswamy, V.G., 1986, "A Constitutive Model for the Inelastic Multiaxial Cyclic Response of a Nickel Base Superalloy RENE 80," NASA CR-3998.

Robinson, D.N., 1984, "Constitutive Relationships for Anisotropic High-Temperature Alloys," Nuclear Engineering and Design, Vol. 83, No. 3, pp. 389-396.

Walker, K.P., and Jordan, E.H., 1987, "Constitutive Modelling of Single Crystal and Directionally Solidified Superalloys," Turbine Engine Hot Section Technology 1987, NASA CP-2493, pp. 299-301.

Dame, L.T., and Stouffer, D.C., 1986, "Anisotropic Constitutive Model for Nickel Base Single Crystal Alloys: Development and Finite Element Implementation," NASA CR-175015.

Robinson, D.N., Duffy, S.F., and Ellis, J.R., 1986, "A Viscoplastic Constitutive Theory for Metal Matrix Composites at High Temperature," NASA CR-179530.

Maffeo, R., 1984, "Burner Liner Thermal-Structural Load Modeling," NASA CR-174892.

McKnight, R.L., 1985, "Component-Specific Modeling," NASA CR-174925.

McKnight, R.L., Chen, P.C., Dame, L.T., Holt, R.V., Hugny, H., Hartle, M., Gellin, S., Allen, D.H., and Haisler, W.E., 1986, "On 3D Inelastic Analysis Methods for Hot Section Components," Turbine Engine Hot Section Technology 1986, NASA CP-2444, pp. 257-268.

Nakazawa, S., 1987, "On 3D Inelastic Analysis Methods for Hot Section Components, Vol. 1 - Special Finite Element Models," NASA CR-179494.

Wilson, R.B. and Banerjee, P.K., 1986, "On 3D Inelastic Analysis Methods for Hot Section Components, Vol. 2 - Advance Special Function Models," NASA CR-179517.

Battiste, R.L. and Ball, S.J., 1986, "Determination of Surfaces of Constant Inelastic Strain Rate at Elevated Temperature," Turbine Engine Hot Section Technology 1986, NASA CP-2444, pp. 307-325.

Bartolotta, P.A. and McGaw, M.A., 1987, "A High Temperature Fatigue and Structures Testing Facility," NASA TM-100151.

Bartolotta, P.A., 1985, "Thermomechanical Cyclic Hardening Behavior of Hastelloy-X," NASA CR-174999.

Ellis, J.R., Bartolotta, P.A., Allen, G.P., and Robinson, D.N., 1986, "Thermomechanical Characterization of Hastelloy-X Under Uniaxial Cyclic Loading," Turbine Engine Hot Section Technology 1986, NASA CP-2444, pp. 293-305.

Bartolotta, P.A., 1987, "Use of Inelastic Strain as a Basis for Analyzing Thermomechanical Test Data," Turbine Engine Hot Section Technology 1987, NASA CP-2493, pp. 303-315.

Ellis, J.R., Bartolotta, P.A., and Mladsi, S.W., 1987, "Preliminary Study of Creep Thresholds and Thermomechanical Response in Haynes 188 at Temperatures in the Range 649 to 871 °C," Turbine Engine Hot Section Technology 1987, NASA CP-2493, pp. 317-334.

Thompson, R.L. and Tong, M.T., 1986, "Unified Constitutive Materials Model Development and Evaluation for High-Temperature Structural Analysis Applications," 15th Congress of the International Council of the Aeronautical Sciences, Vol. 2, AIAA, New York, pp. 1505a-1505s.

TABLE I. - HOST STRUCTURAL ANALYSIS PROGRAMS

NAS3-23925, Southwest Research Institute (U.S. Lindholm), Constitutive Modeling for Isotropic Materials.

NAS3-23927, General Electric (V.G. Ramaswamy), Constitutive Modeling for Isotropic Materials.

NAS3-379, University of Akron (D.N. Robinson), Multiaxial Theories of Viscoplastic for Isotropic and Anisotropic Materials.

NAG3-512, University of Connecticut (E.H. Jordan), Constitutive Modeling of Single Crystal and Directionally Solidified Superalloys.

NAG3-511, University of Cincinnati (D.C. Stouffer), Anisotropic Constitutive Modeling for Nickel-Base Single Crystal Superalloy René N4.

NAS3-23272, General Electric (R. Maffeo), Burner Liner Thermal/Structural Load Modeling.

NAS3-23687, General Electric (R.L. McKnight), Component-Specific Modeling.

NAS3-23698, General Electric (R.L. McKnight), Three-Dimensional Inelastic Analysis Methods for Hot Section Components I.

NAS3-23697, Pratt and Whitney Aircraft (E.S. Todd), Three-Dimensional Inelastic Analysis Methods for Hot Section Components II.

IAN 40-1447-84 and DE-AC05-840R 21400, Oak Ridge National Laboratory (J.R. Corum), Determination of Surface of Constant Inelastic Strain Rate at Elevated Temperature.

NASA Lewis Research Center (J.R. Ellis and P.E. Moorhead), High-Temperature Fatigue and Structures Laboratory/Structural Component Response Facility.

TABLE II. - CREEP THRESOLDS DETERMINED FOR HAYNES 188 AT TEMPERATURES IN THE RANGE 649 TO 871 °C

Temperature, °C	Creep thresold,[a] ksi
649	30
760	11
871	4

TABLE III. - SUMMARY OF STRUCTURAL-LIFE ANLAYSES OF COMBUSTOR LINERS AT A CRITICAL LOCATION

(a) Conventional liner

Analytical method	Temperature range, °F	Strain range, με		Mean stress, psi	Predicted life, cycles
		Mechanical	Inelastic		
Unified (Walker)	950 to 1630	5870	3150	-35 000	400 to 1000
Unified (Bodner)	950 to 1630	5800	2700	-28 000	400 to 1000

(b) Segmented liner

Analytical method	Temperature range, °F	Strain range, με		Mean stress, psi	Predicted life, cycles
		Mechanical	Inelastic		
Unified (Walker)	755 to 1180	810	10^{-1}	10 000	$>10^6$
Unified (Bodner)	755 to 1180	820	10^{-1}	15 000	$>10^6$

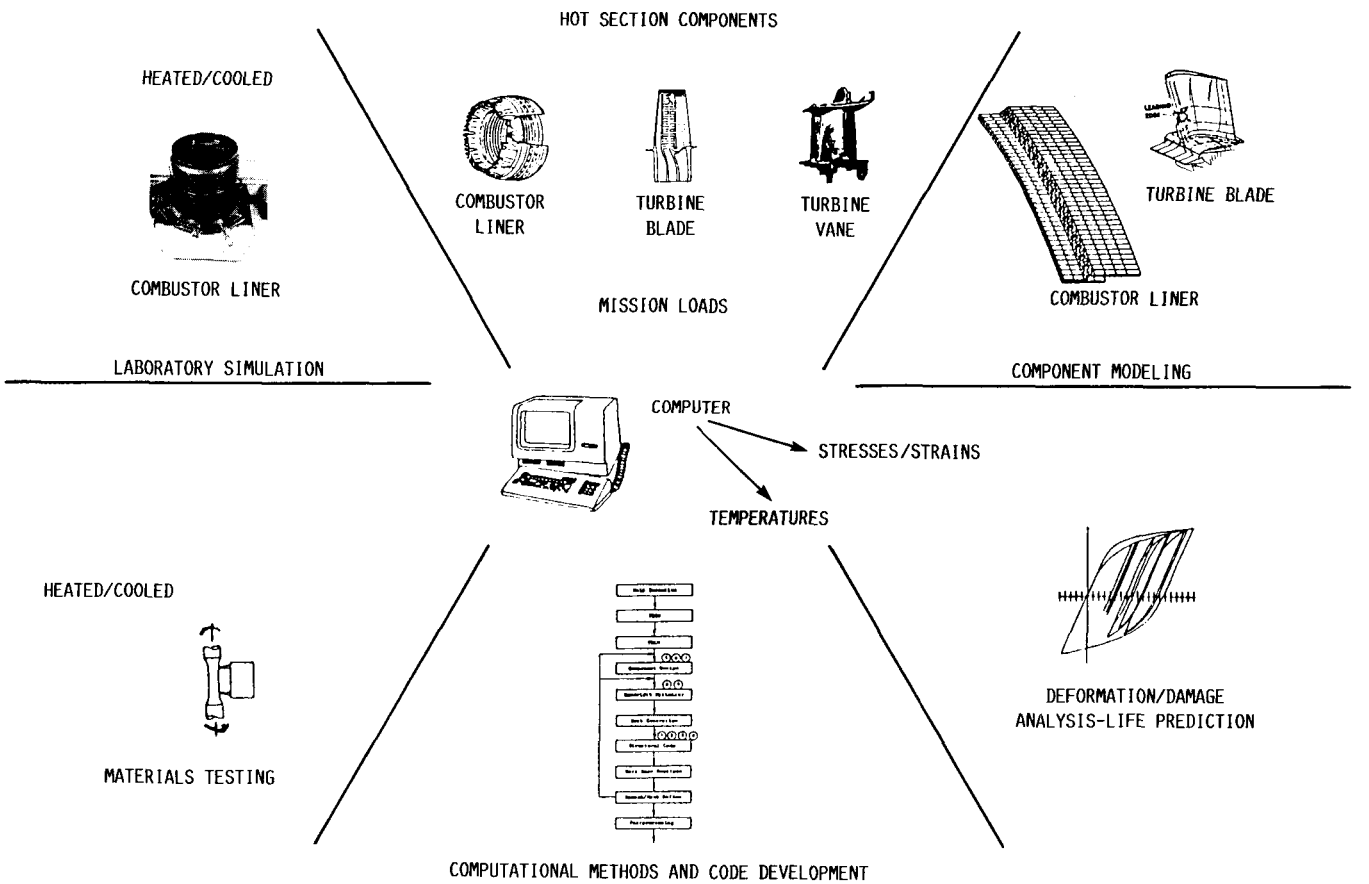

FIGURE 1. - NONLINEAR STRUCTURAL ANALYSIS TECHNOLOGIES AND ACTIVITIES UNDER HOST.

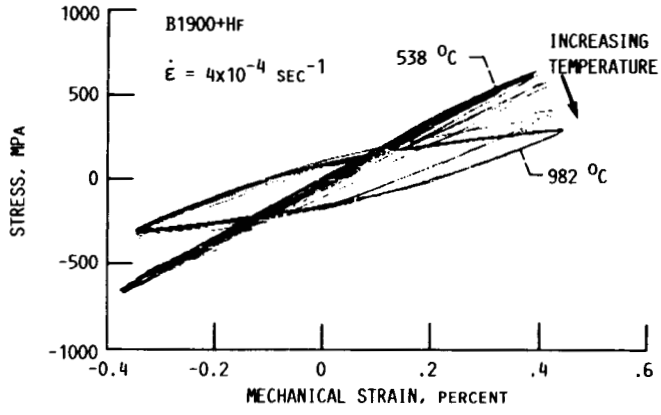

FIGURE 2. - CONTROLLED STRAIN CYCLING WITH TEMPERATURE CHANGE FROM 538 °C TO 982 °C.

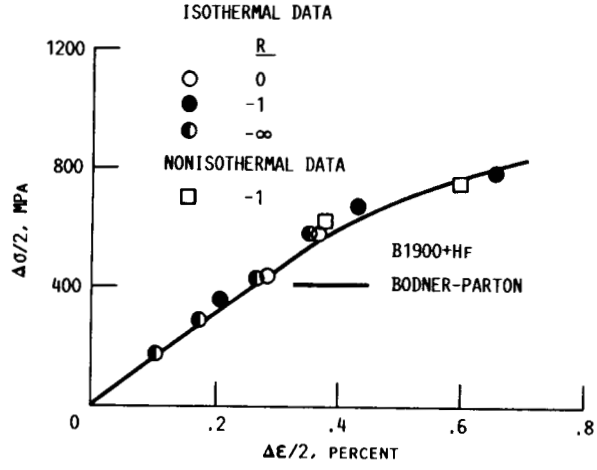

FIGURE 3. - COMPARISON OF ISOTHERMAL AND NON-ISOTHERMAL CYCLIC DATA OF B1900+Hf AT 760 °C.

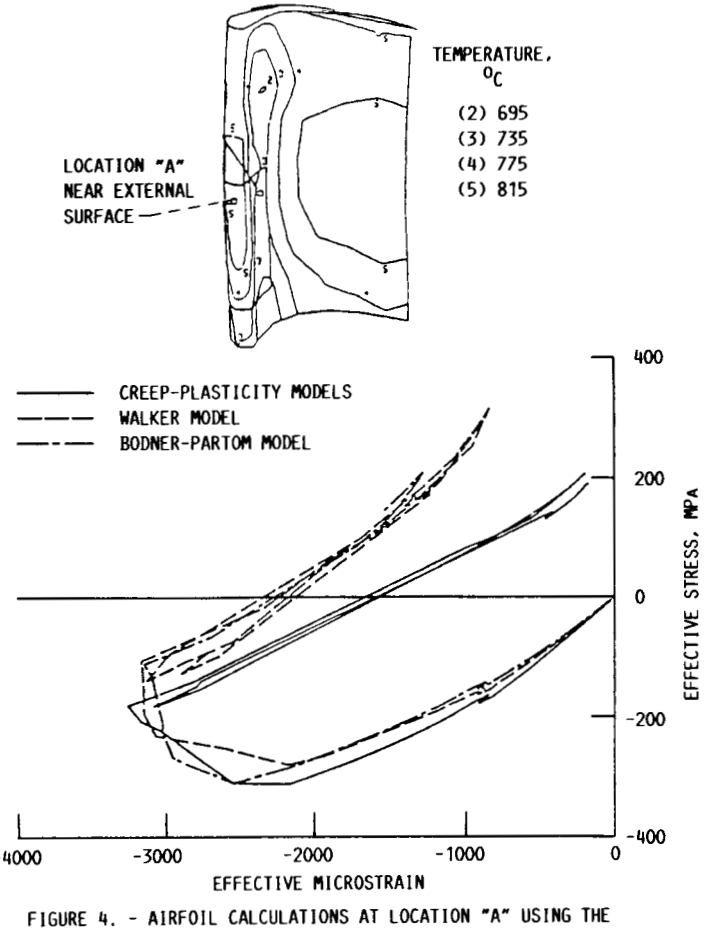

FIGURE 4. - AIRFOIL CALCULATIONS AT LOCATION "A" USING THE MARC FINITE ELEMENT ANALYSIS CODE.

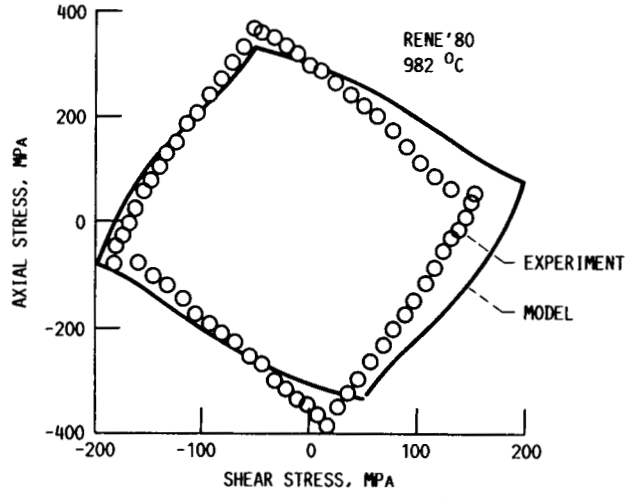

FIGURE 5. - RENE'80 RESPONSE TO 90° OUT-OF-PHASE TENSION/TORSION CYCLIC LOADING.

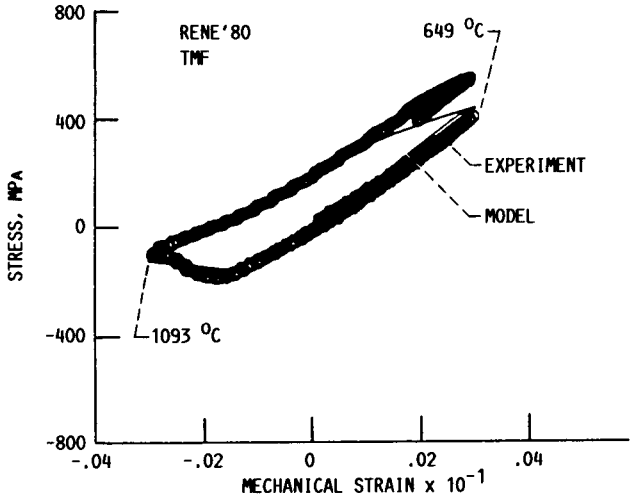

FIGURE 6. - RENE'80 TMF RESPONSE (649-1093 °C OUT-OF-PHASE).

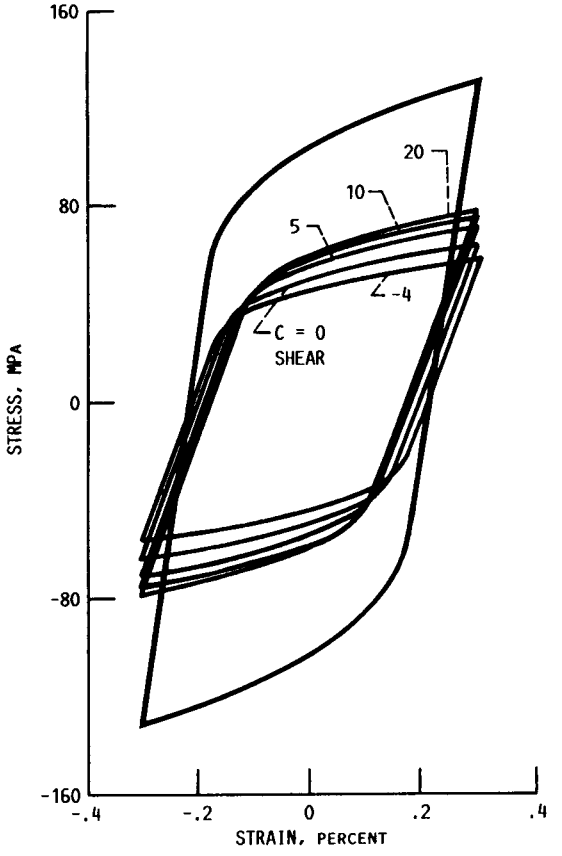

FIGURE 7. - SATURATED HYSTERESIS LOOPS FOR $\Delta\epsilon$ = 0.6 PERCENT AND $\dot{\epsilon}$ = .001/M. SHOWN IS UNIAXIAL RESPONSE AND SHEAR RESPONSES FOR SEVERAL VALUES OF C.

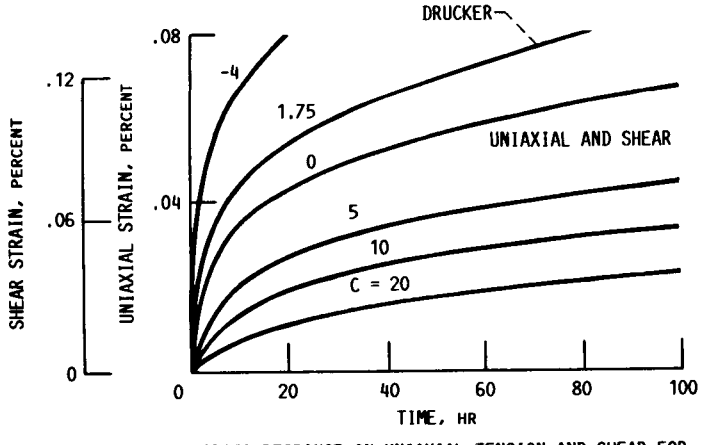

FIGURE 8. - CREEP RESPONSE IN UNIAXIAL TENSION AND SHEAR FOR SEVERAL VALUES OF C.

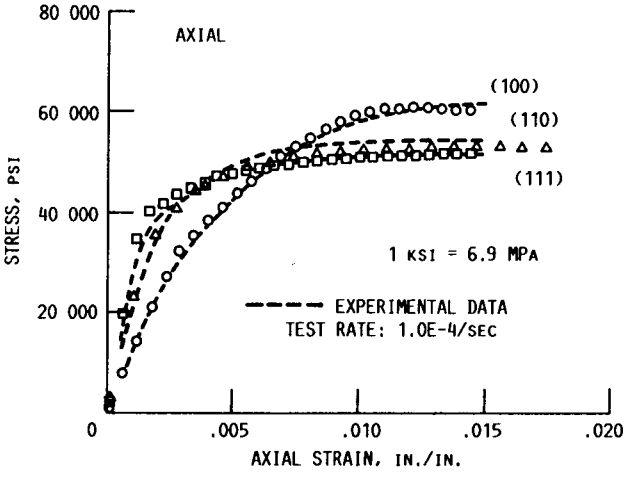

FIGURE 9. - RENE N4 PREDICTED TENSILE RESPONSE AND EXPERIMENTAL DATA FOR SPECIMEN ORIENTATIONS OF [100], [110], AND [111] AT 982 °C (1800 °F).

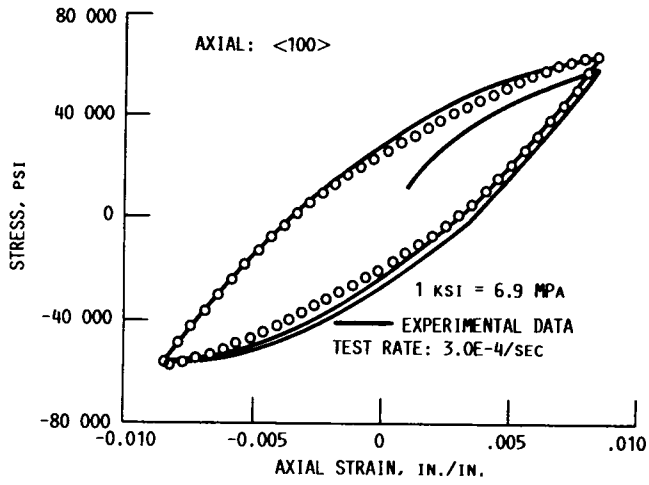

FIGURE 10. - RENE N4 PREDICTED CYCLIC RESPONSE AND EXPERIMENTAL DATA FOR SPECIMEN ORIENTATION OF [100] AT 982 ^{o}C (1800 ^{o}F).

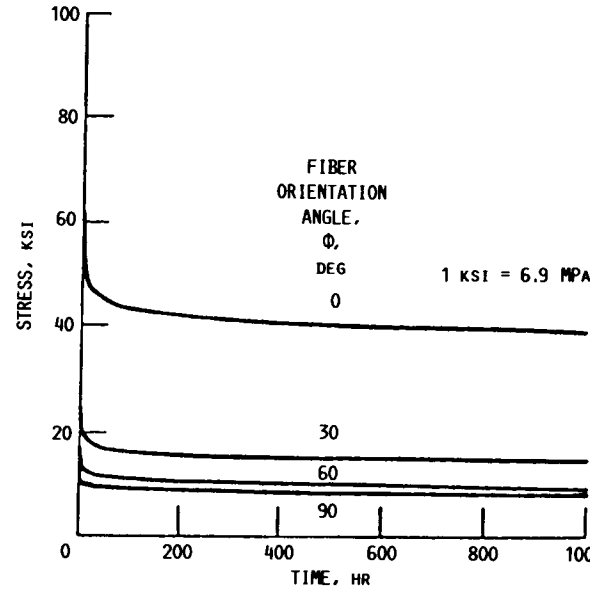

FIGURE 11. - RELAXATION CURVES FOR DIFFERENT FIBER ORIENTATION ANGLES.

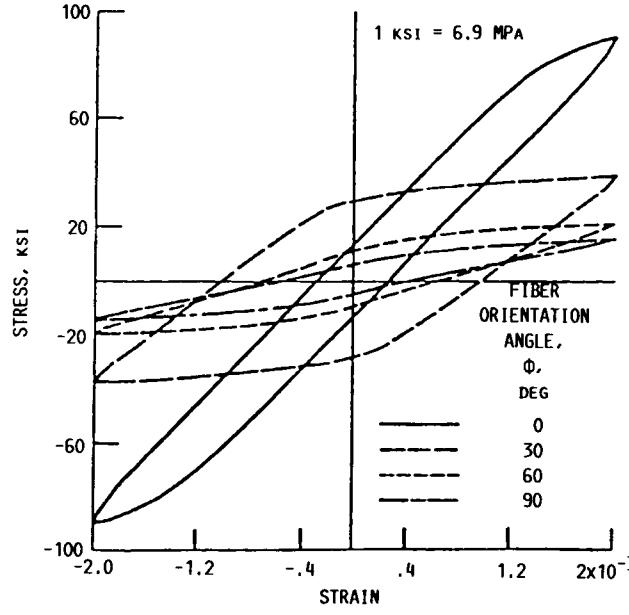

FIGURE 12. - HYSTERESIS LOOPS FOR DIFFERENT FIBER ORIENTATION ANGLES; STRAIN RATE = 0.001/MIN.

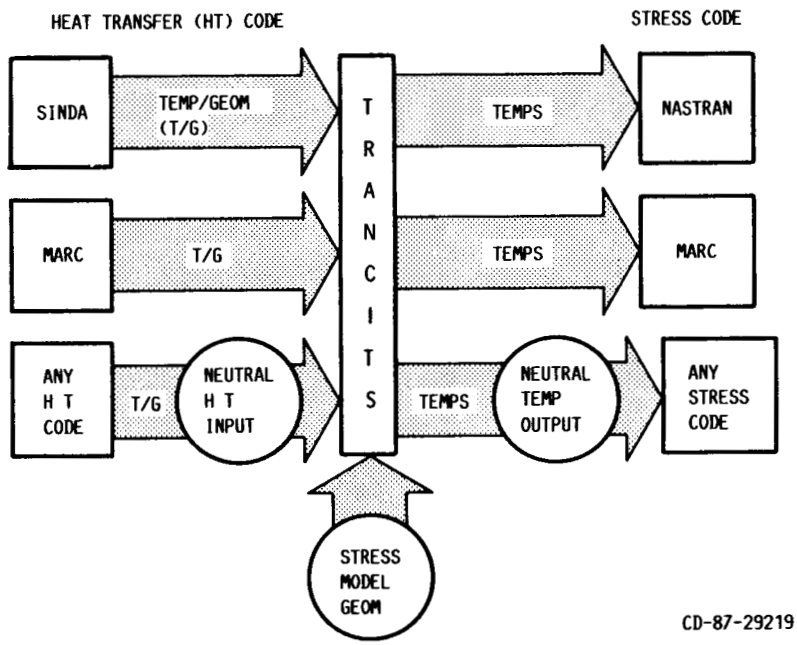

FIGURE 13. - SCHEMATIC FOR THREE-DIMENSIONAL TRANCITS COMPUTER PROGRAM.

COMBUSTOR LINER PARAMETER LIST

CODE	NAME	DEFAULT	CODE	NAME	DEFAULT
1	X_1	0.0	2	Y_1	0.0
3	σ_1	0.0	4	L_1	10.5
5	L_2	2.0	6	L_3	0.5
7	L_4	6.0	8	L_5	0.8
9	L_6	1.0	10	L_7	2.0
11	T_1	0.5	12	T_2	0.7
13	T_3	0.5	14	T_4	0.65
15	T_5	0.5	16	θ_1	90.0
17	θ_2	90.0	18	R_1	1.0
19	R_2	1.0	20	R_3	0.75
21	R_4	1.5	22	R_5	1.5
23	R_6	1.5			

X = COORDINATE
Y = COORDINATE
σ = ANGLE WRT. x - AXIS
L = LENGTH
T = THICKNESS
θ = ANGLE OF ROTATION
R = RADIUS OF CURVATURE
(N) = PARAMETER CODE NUMBER

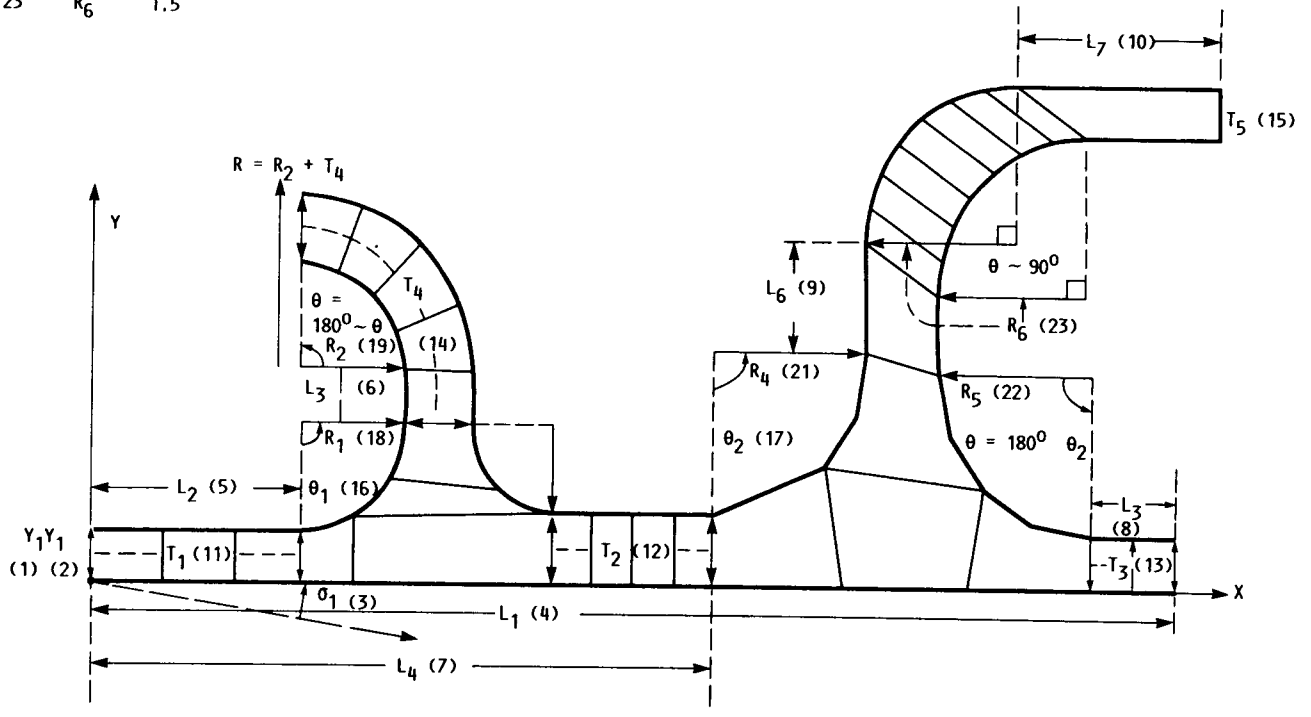

FIGURE 14. - COMBUSTOR LINER PARAMETERS.

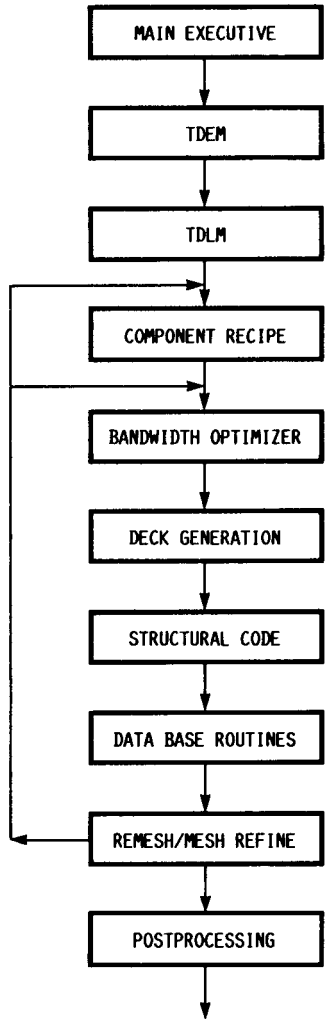

FIGURE 15. - SYSTEM FLOW CHART FOR COSMO.

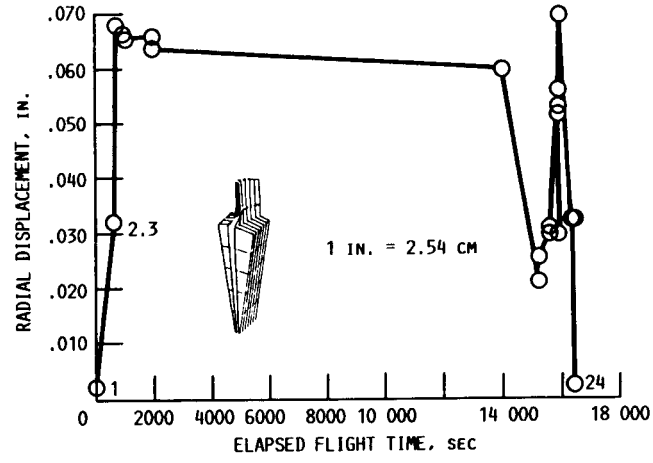

FIGURE 16. - RADIAL DISPLACEMENT OF LEADING EDGE TIP, STATIC.

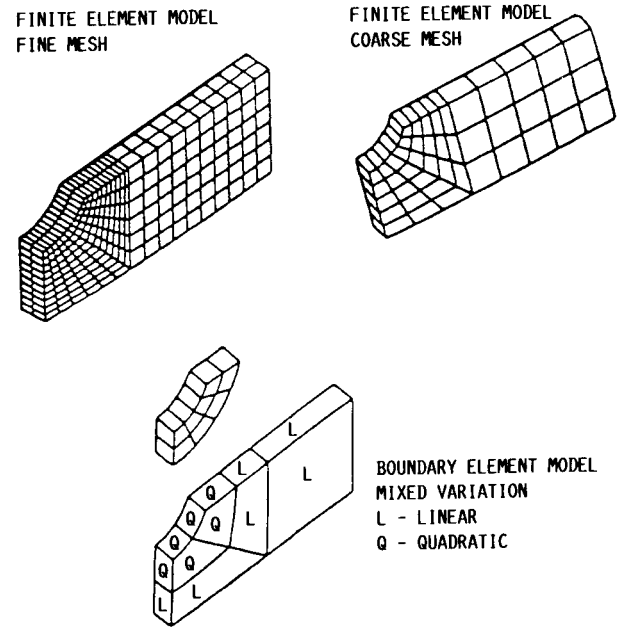

FIGURE 17. - MESHES USED IN BENCHMARK NOTCH ANALYSIS.

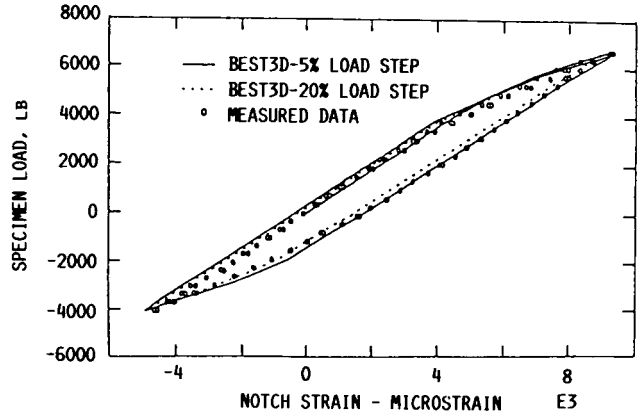

FIGURE 18. - CYCLIC BEHAVIOR AT ROOT OF SPECIMEN NOTCH.

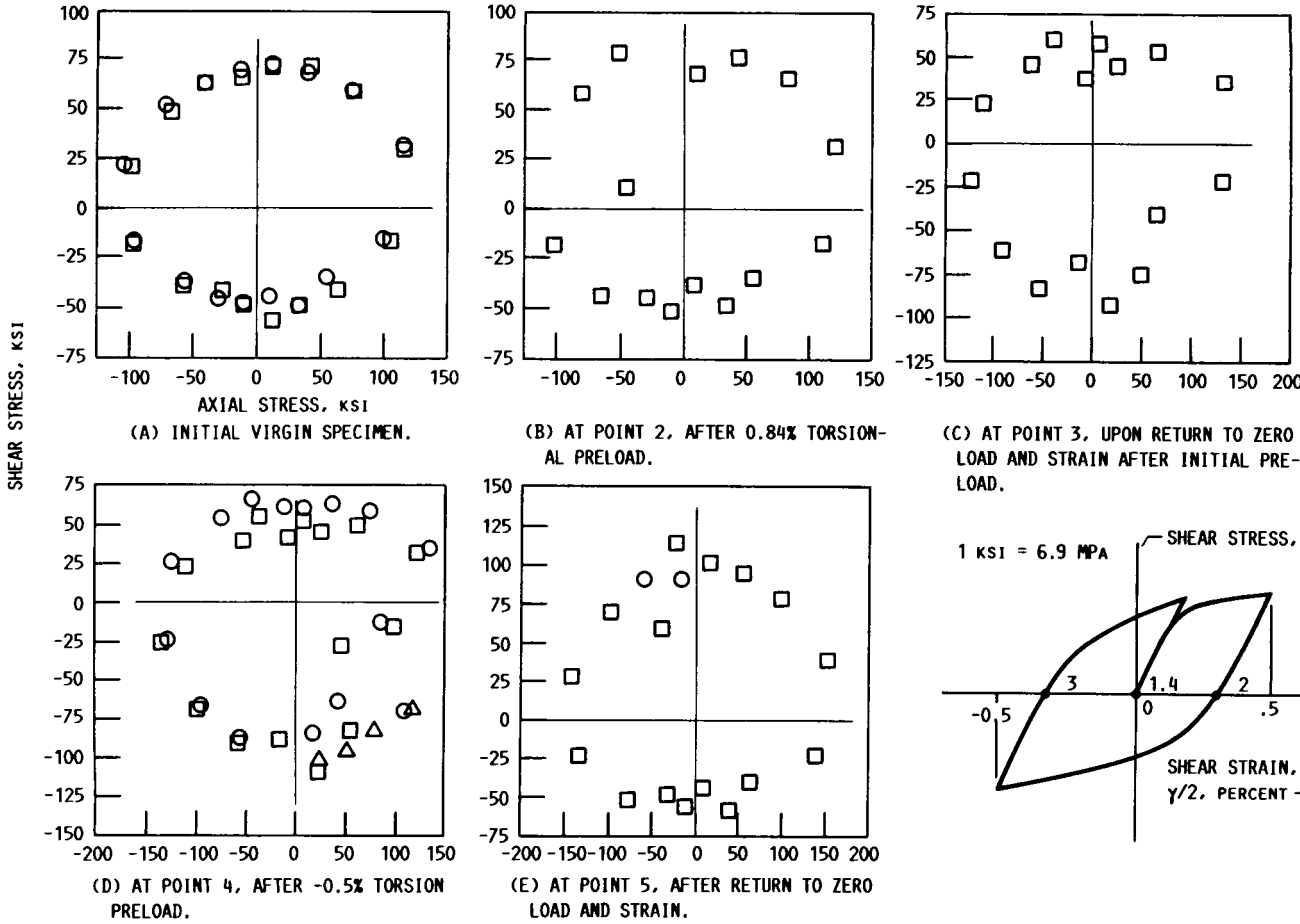

FIGURE 19. - MEASURED 650 ^{o}C SURFACES OF CONSTANT INELASTIC STRAIN RATE FOR REFERENCE SCISRs TEST PROGRAM.

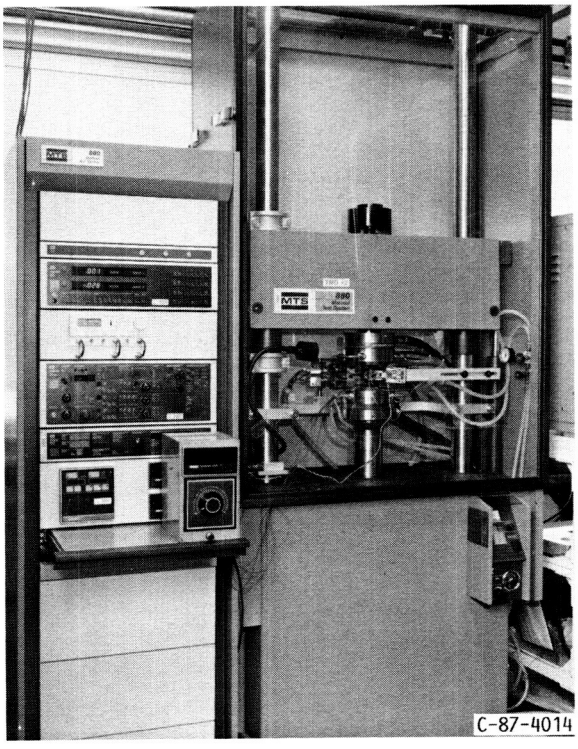

UNIAXIAL TEST SYSTEM

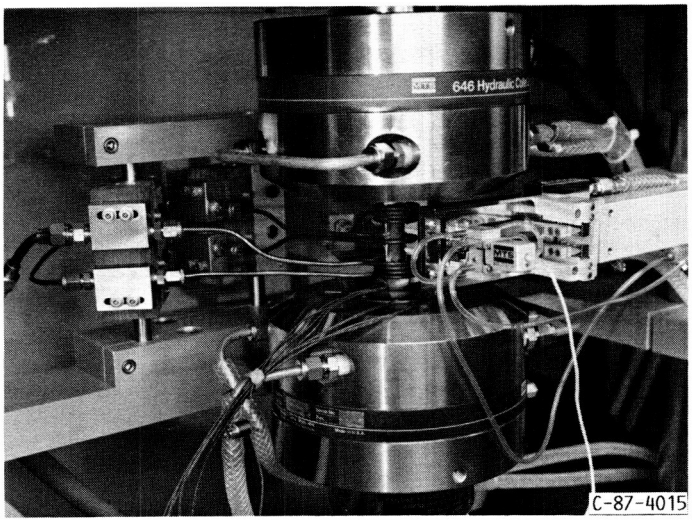

UNIAXIAL LONGITUDINAL EXTENSOMETER IN TEST SETUP

FIGURE 20. - UNIAXIAL TEST SYSTEM.

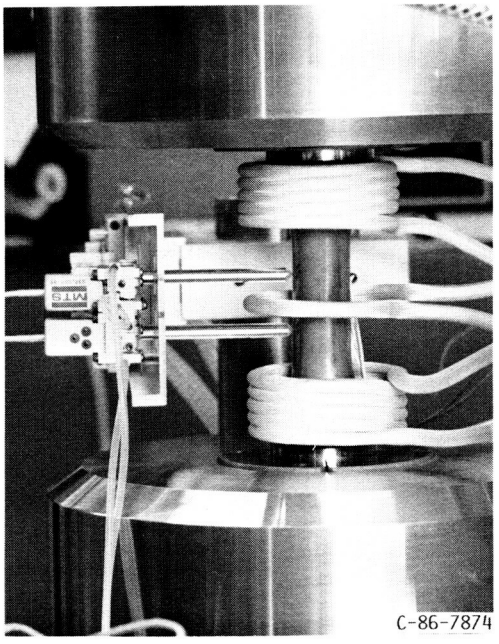

COMMERCIALLY AVAILABLE BIAXIAL EXTENSOMETER

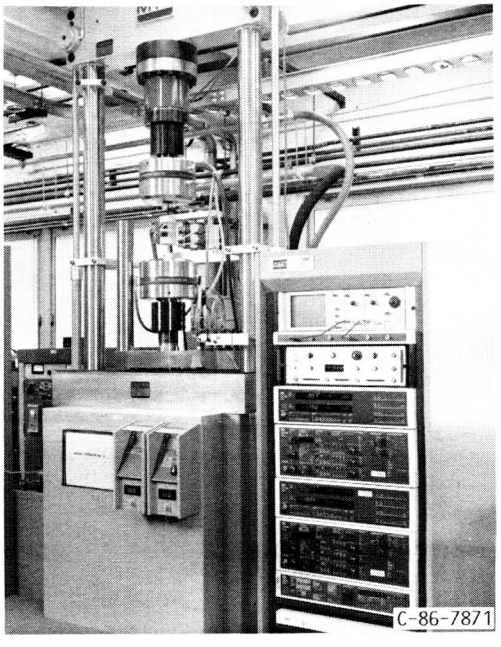

BIAXIAL MATERIAL TEST SYSTEM

FIGURE 21. - BIAXIAL MATERIAL TEST SYSTEM.

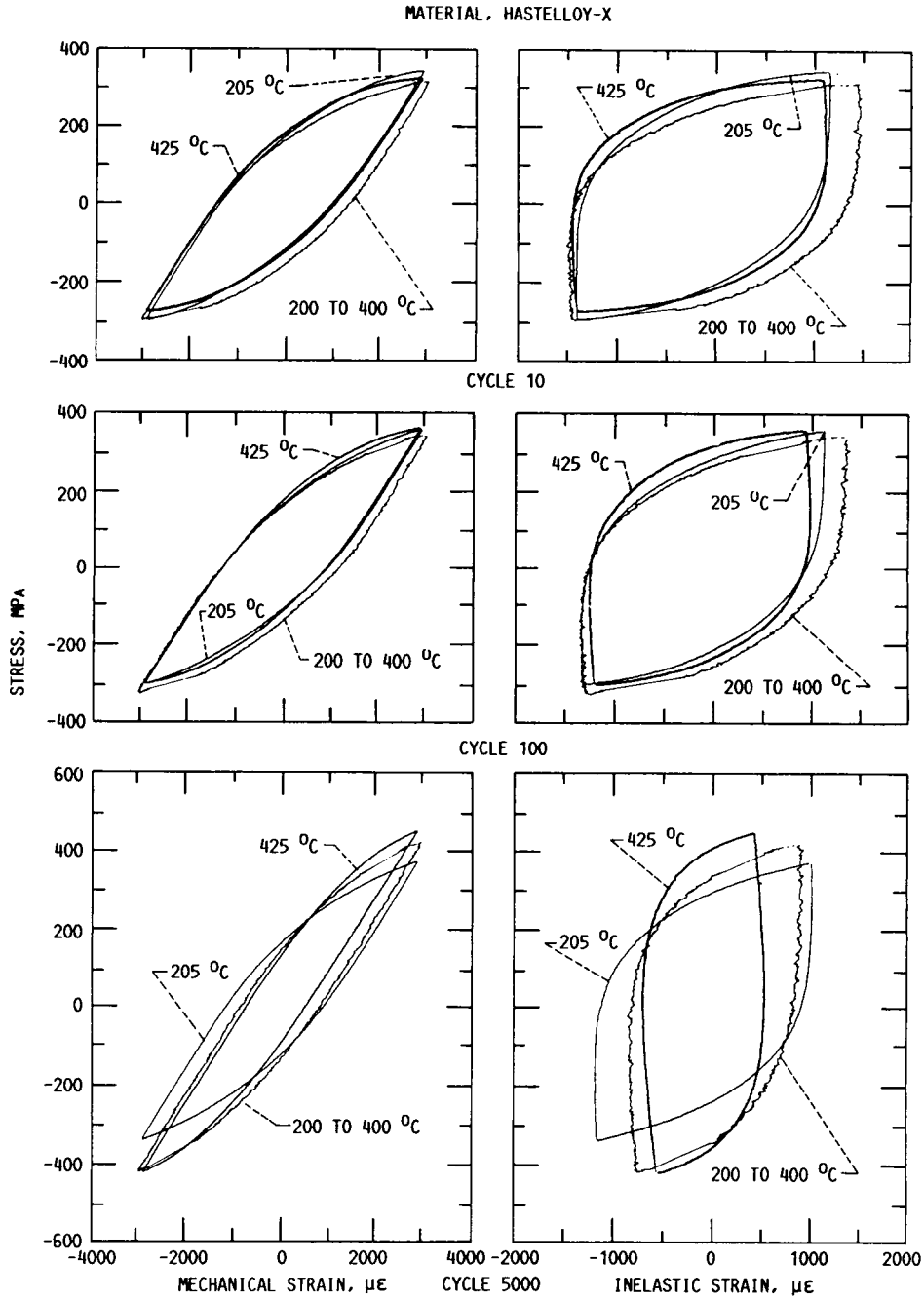

FIGURE 22. - COMPARISON OF MATERIAL RESPONSE DETERMINED UNDER ISOTHERMAL AND THERMO-MECHANICAL CYCLIC LOADING.

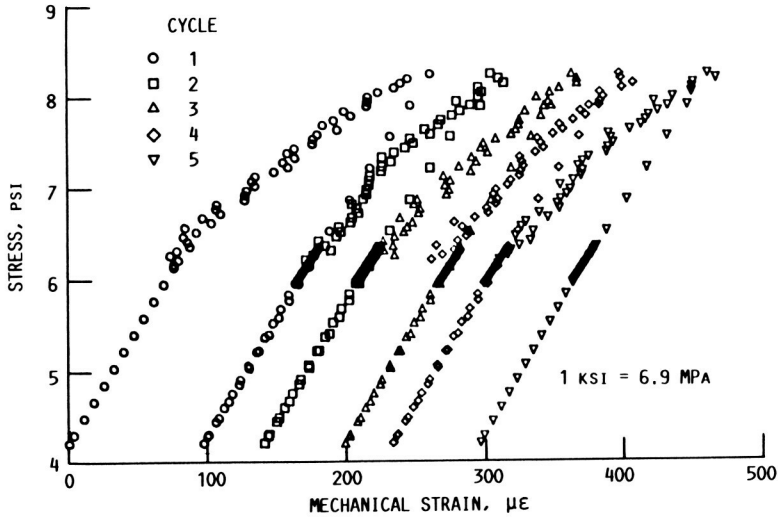

FIGURE 23. - CREEP RATCHETTING RESULTING FROM THERMOMECHANICAL CYCLING FOR 6.17 KSI MEAN STRESS.

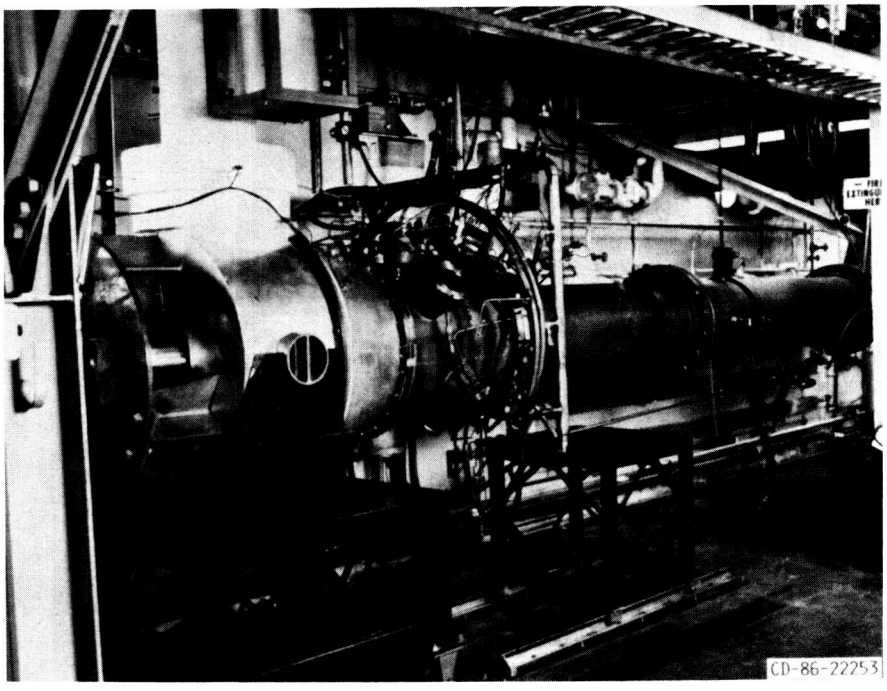

FIGURE 24. - STRUCTURAL COMPONENT RESPONSE RIG.

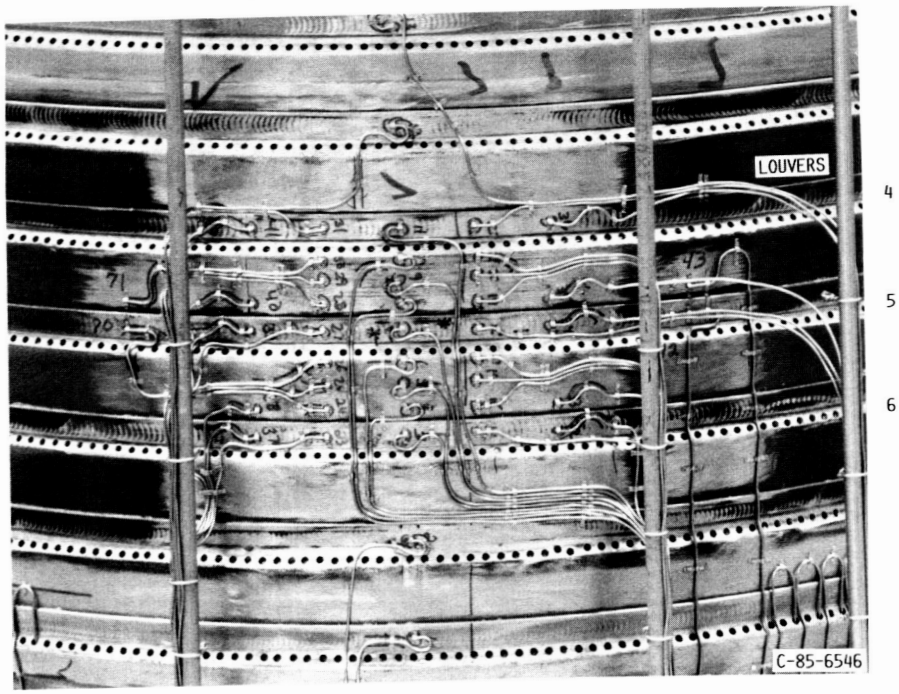

CONVENTIONAL

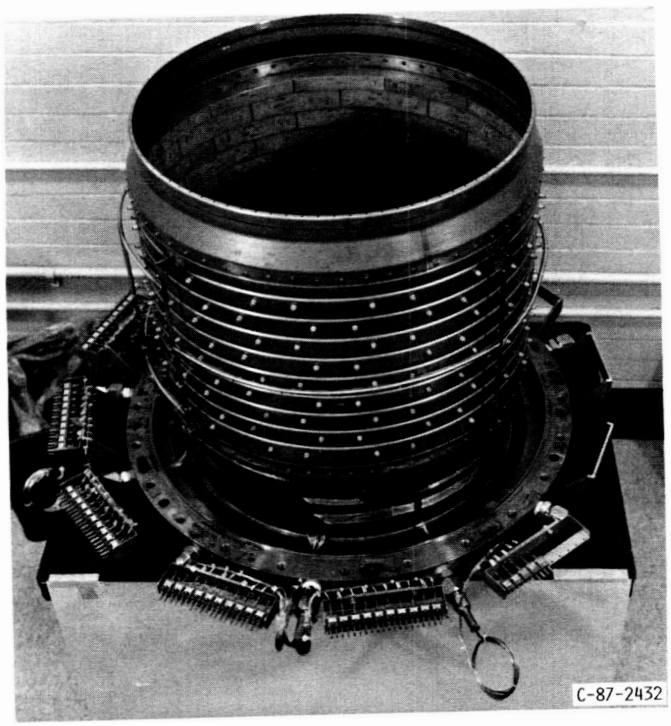

ADVANCED (SEGMENTED)

FIGURE 25. - CONVENTIONAL AND SEGMENTED COMBUSTOR LINERS INSTRUMENTED FOR TESTING.

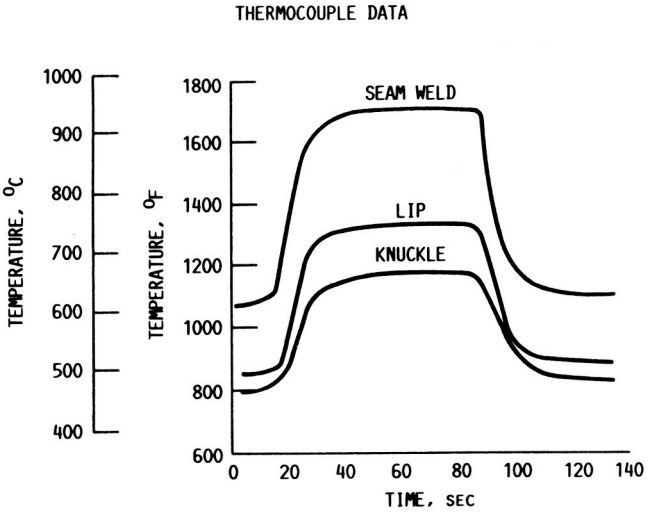

FIGURE 26. - CYCLIC SURFACE LINER TEMPERATURES AT THREE LOCATIONS ON LOUVER 5.

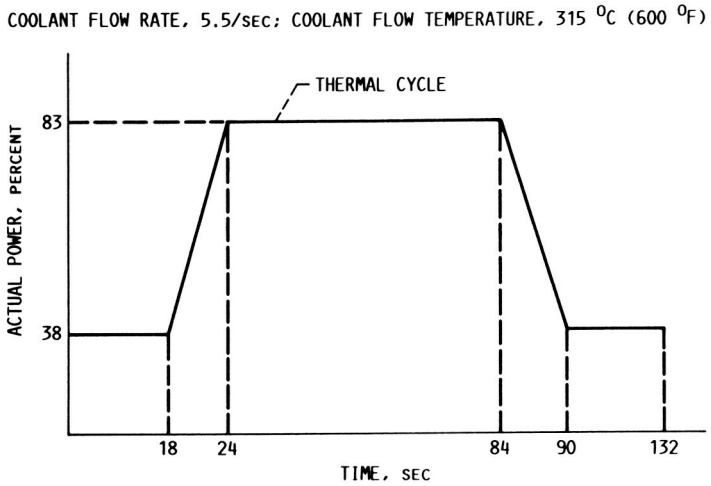

FIGURE 27. - POWER HISTORY FOR THERMAL CYCLE.

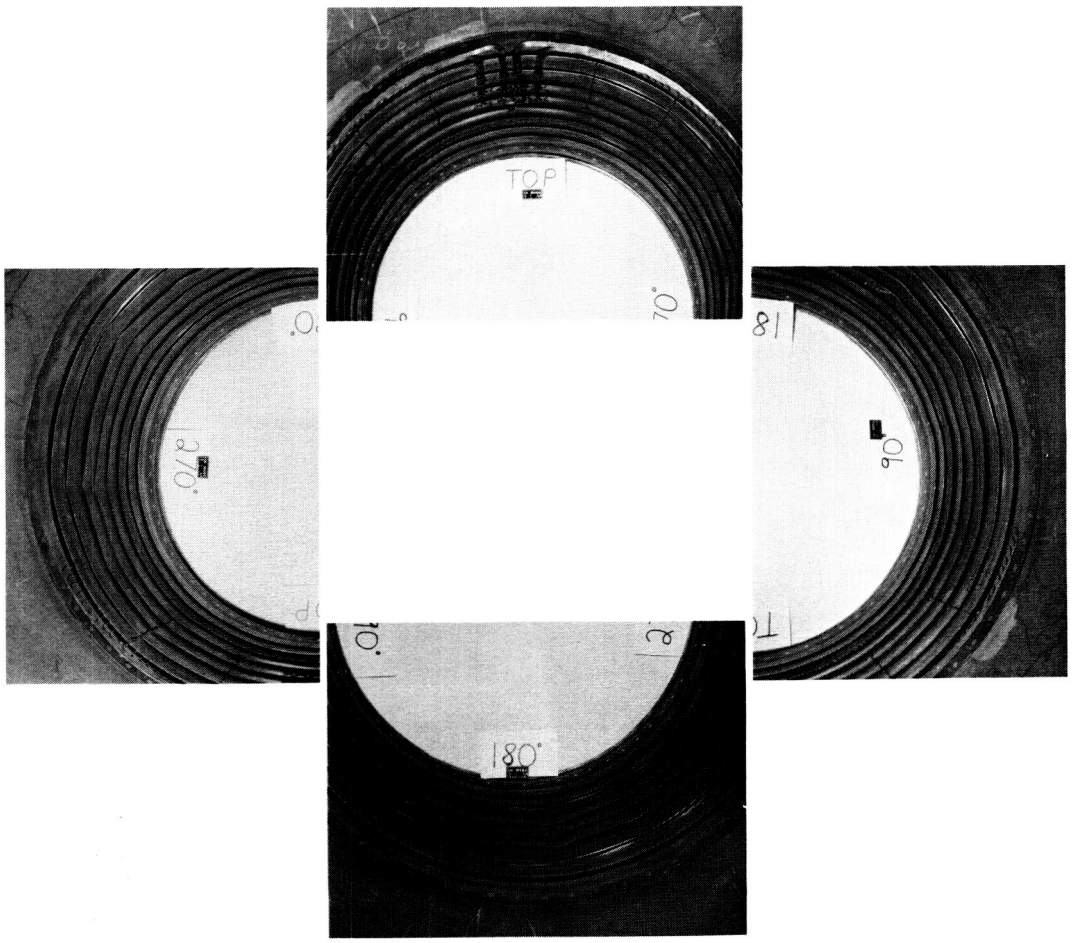

FIGURE 28. - COMPOSITE PHOTOGRAPH OF HOT SIDE CONVENTIONAL LINER DISTORTION AFTER 1782 THERMAL CYCLES.

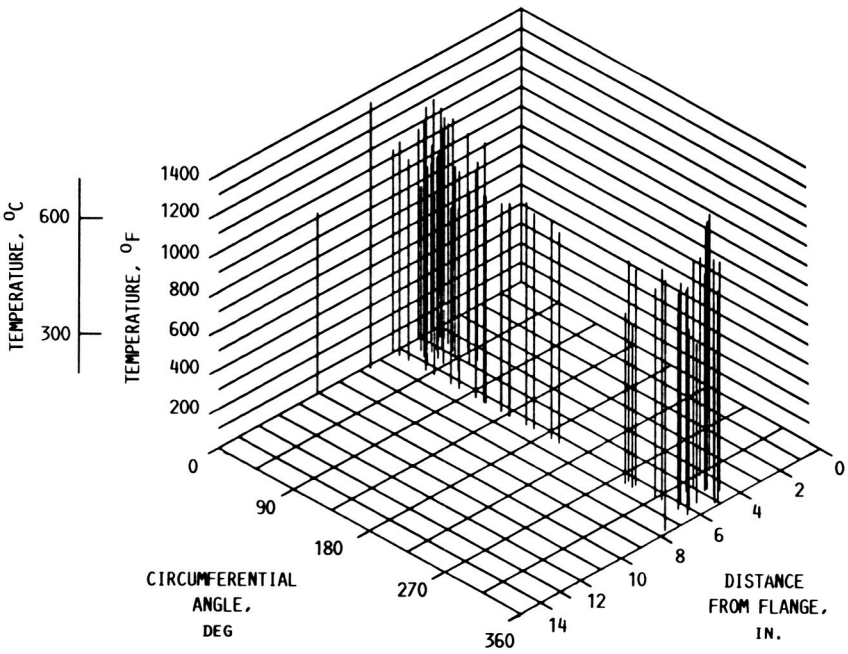

FIGURE 29. - ISOMETRIC PLOT OF TEMPERATURE ON INSIDE OF SEGMENTED COMBUSTOR LINER.

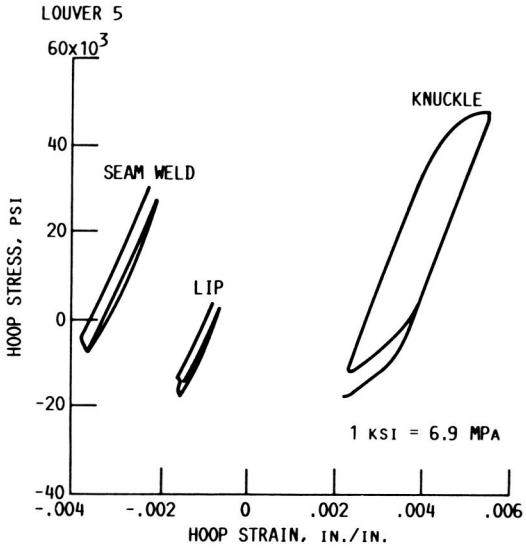

FIGURE 30. - REPRESENTATIVE STRESS-STRAIN PREDICTIONS AT THREE LOCATIONS ON THE CONVENTIONAL LINER.

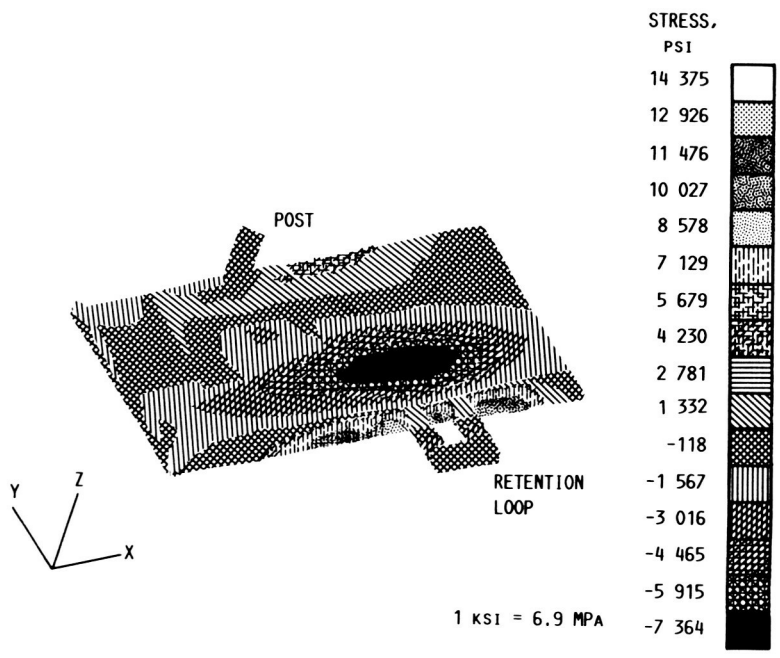

FIGURE 31. - ADVANCED COMBUSTOR LINER STRESS DISTRIBUTION ON SYMMETRICAL PANEL AT AN 83 PERCENT POWER LEVEL (X-DIRECTION).